Origami Engineering

Diego Misseroni[1,a], **Phanisri P. Pratapa**[1,b], **Ke Liu**[1,c], **Biruta Kresling**[d], **Yan Chen**[e], **Chiara Daraio**[f], **Glaucio H. Paulino**[g,h,*]

[a] Department of Civil, Environmental and Mechanical Engineering, University of Trento, Trento 38123, Italy

[b] Department of Civil Engineering, Indian Institute of Technology Madras, Chennai 600036, TN, India

[c] Department of Advanced Manufacturing and Robotics, Peking University, Beijing 100871, China

[d] Experimental Design and Bionics, 75015 Paris, France

[e] School of Mechanical Engineering, Tianjin University, Tianjin, 300350, China

[f] Division of Engineering and Applied Science, California Institute of Technology, Pasadena, 91125, CA, USA

[g] Department of Civil and Environmental Engineering, Princeton University, Princeton, New Jersey, 08544, USA

[h] Princeton Materials Institute (PMI), Princeton University, Princeton, New Jersey, 08544, USA

Editor: **Natalie Barnes** (natalie.barnes@nature.com)
Nature Reviews Methods Primers (NRMP)
*Corresponding author: email: gpaulino@princeton.edu
[1] Equal contributing author
Red text: Glossary

Abstract

Origami traces its origins to an ancient art form transforming flat thin surfaces into various complex, fabulous three-dimensional objects. Nowadays, such transformation transcends art by offering a conceptual framework for non-destructive and scale-independent abstractions for engineering applications across diverse fields with potential impact in education, science, and technology. For instance, a growing number of architected materials and structures are based on origami principles, leading to unique properties that are distinct from those previously found in either natural or engineered systems. To disseminate those concepts, this Primer provides a comprehensive overview of the major principles and elements in origami engineering, including theoretical fundamentals, simulation tools, manufacturing techniques, and testing protocols that require non-standard setups. We highlight applications involving deployable structures, metamaterials, robotics, medical devices, and programmable matter to achieve functions such as vibration control, mechanical computing, and shape morphing. We identify challenges for the field, including finite rigidity, panel thickness accommodation, incompatibility with regular mechanical testing devices, manufacturing of non-developable patterns, sensitivity to imperfections, and identifying the relevant physics at the scale of interest. We further envision the future of origami engineering aimed at next-generation multifunctional material and structural systems.

[H1] Introduction

Origami, the ancient art of paper folding, has proven to be a powerful concept, inspiring innovations in science, engineering, and beyond. Reflecting on the famous quote by Louis Sullivan, "form follows function," it becomes clear how the power of folding, with its ability to transform one geometric form to another (from 2D to 3D in most cases), is essential. This transformation creates new possibilities for scientists and engineers to design multifunctional machines, lightweight structures and architected materials (see Table 1). The ideas of folding induced origami structures can be found in nature[1] (see Figure 1A), and in thin walled structures undergoing sudden large deformation (see Figure 1B,C)[2,3]. A recent noteworthy engineering application of origami is the starshade structure, which is illustrated in Figure 1D.

Mathematically, an origami is locally a two-dimensional, discrete manifold, which is characterized simply by a set of creases, namely lines on the manifold where (sharp) folding occurs; and folding angles of the creases that determines the amount of folding. The creases divide the manifold into two-dimensional pieces, which are called panels. The creases can either be straight or curved lines. When all the creases are straight lines, the panels are polygonal in shape[4]. The points of intersection of the creases are referred to as the vertices. The local structure of an origami refers to any portion of the origami that is away from boundaries and intersections of multiple (>2) panels. It is possible that some origami do not have any boundary, forming enclosed polyhedra. In the remainder of this Primer, unless otherwise stated, origami refers to patterns with straight creases and thin panels.

Depending on the direction of the crease that the folding action is pushing it to, creases are categorized as mountain (M) folds and valley (V) folds. In other words, the mountain/valley (M/V) assignment of a crease determines whether it folds up (mountain) or down (valley). The M/V assignments are relative because depending on the viewing angle, mountain folds can be viewed as valley folds, and vice versa, but they are always pointing to opposite directions (locally). Such a convention leads to the crease pattern, a blueprint for origami structures, as shown in Figure 1E. Next, let us first introduce a few frequently studied properties in origami-related research articles, as they govern the mechanical and kinematic behavior of origami structures.

[H2] Developability

Following the instruction of the crease pattern, typical origami folds up from a flat sheet into a 3D shape through isometric, or nearly isometric transformation, without subjecting the sheet to stretch or tearing. Such an origami structure, with a flat initial state, is called developable (for example, the Miura-ori pattern). Theoretically, when the thickness of the sheet is assumed to be zero, the volume encompassed by the origami structure in its developed state is zero. To determine whether an origami is locally developable from its crease pattern, the N panel angles (for example, $\{\alpha_i, i = 1..N\}$), or sector angles, meeting at a vertex can be added up. If their sum is 360 degrees (or 2π), this vertex can be flattened onto a plane (see Figure 1F). Mathematically, this condition is expressed as:

$$\alpha_1 + \alpha_2 + \alpha_3 + \cdots + \alpha_N = 2\pi$$

If all vertices of an origami are developable, this origami is globally developable. We note that this rule only applies to vertices with neighborhoods that are locally two-dimensional manifold.

[H2] Flat foldability

When the folding-induced transformation includes a state (other than the developed state) in which the entire origami structure can be flattened onto a plane, typically with overlapping of panels, the corresponding origami is called flat-foldable (for example, the Miura-ori pattern). The folded planar state is referred to as the flat-folded state. In general, there may be more than one flat-folded states for an origami. The *Kawasaki-Justin theorem* gives the locally necessary and sufficient condition for an origami vertex to be flat-foldable. For an origami vertex with *N* consecutive panel angles (*N* must be even) labelled from 1 to *N* (Figure 1G), then the vertex can be flat-foldable if:

$$\alpha_1 - \alpha_2 + \alpha_3 - \alpha_4 \ldots - \alpha_N = 0$$

The number *N* is called the degree of a vertex, defined as the number of creases incident on a vertex. The *Kawasaki-Justin theorem* deals with the panel angles but do not guide how an origami vertex can be folded flat, which relates to the *M/V* assignment (see Figure 1H). The condition about fold directions for a flat-foldable vertex is the *Maekawa-Justin Theorem*:

Let M be the number of mountain folds and V be the number of valley folds. If an origami vertex is flat foldable, then

$$M - V = \pm 2 \, .$$

The Maekawa-Justin theorem is a locally necessary but not sufficient condition. For a crease pattern to be globally flat-foldable, all of its vertices must be locally flat-foldable, which is still, a necessary but not sufficient condition. Any flat foldable vertex must have even degrees (precondition of *Kawasaki-Justin theorem*), which leads to a necessary criterion for global flat-foldability: the 2-colorability of a crease pattern (see Figure 1E). A graph with all even degree vertices can be called an Eulerian graph, and it has been proven that Eulerian graphs satisfy 2-face-coloring[5]. However, "flat-foldability is hard" (NP-hard, indeed) [6]. The readers are referred to references[6,7] for more details. It is noted that flat foldability is a new, independent property from developability, for example, the eggbox is not developable but flat-foldable.

[H2] Rigid foldability

During the folding-induced transformation, if the deformation of the sheet is only concentrated along the creases, without bending or stretching the panels, this origami is called rigid origami. It means that the origami can be folded while keeping all regions of the paper flat and all crease lines straight[5]. Along with the emergence of origami engineering, analysis of rigid foldability became of great interest in the first two decades of the 21st century. This is because of the increasing use of new materials other than paper for origami applications. While paper is quite forgiving if the panels must deform, other materials, such as metal, wood, and stiff plastics are not. The well-known Miura-ori pattern, eggbox pattern, waterbomb pattern, Yoshimura pattern are all rigid origami, but the square twist[8,9] and Hypar[10] patterns are not rigid origami.

A necessary but not sufficient condition for rigid foldability given a single origami vertex[11,12] specifies that the product of rotation matrices about all the creases (say N in number) of a vertex should be the identity matrix ($\mathbf{I}$)[13,14], using the Belcastro-Hull theorem:

$$\prod_{i=1}^{N} \mathbf{R}_{\rho}\,(\rho_i)\,\mathbf{Q}_{\alpha}(\alpha_i) = \mathbf{I}$$

where $\mathbf{R}_{\rho}$ and $\mathbf{Q}_{\alpha}$ are the transformation matrices in terms of the turning angles ρ_i and panel angles α_i, respectively (see Figure 1I). These matrices are given by:

$$\mathbf{R}_{\rho}(\rho_i) = \begin{bmatrix} 1 & 0 & 0 \\ 0 & \cos\rho_i & -\sin\rho_i \\ 0 & \sin\rho_i & \cos\rho_i \end{bmatrix}, \qquad \mathbf{Q}_{\alpha}(\alpha_i) = \begin{bmatrix} \cos\alpha_i & -\sin\alpha_i & 0 \\ \sin\alpha_i & \cos\alpha_i & 0 \\ 0 & 0 & 1 \end{bmatrix}$$

As an application of the above condition, we consider the degree-4 vertex shown in Figure 1I. In this example, N=4 and if we choose $\alpha_1 = \alpha_4 = 60°$ and $\alpha_2 = \alpha_3 = 120°$ then for a particular partially folded state, the turning angles are $\rho_1 \approx -53.13°$, $\rho_2 = \rho_4 = 90°$ and $\rho_3 \approx 53.13°$. The sign of the turning angle is obtained by using the right-hand thumb rule with the thumb pointing along each of the creases in a consistent direction (either inward or outward from the vertex) as the fingers curl along the arrows marked for ρ_i, as shown in Figure 1I. If the direction of the thumb has to change in order to follow the arrow marked for a turning angle, then it suggests a change of sign. Using these choices of angles, it can be shown that the product of the rotation matrices about all the four creases would be an identity matrix.

The matrix approach is quite practical and useful when analyzing origami structures with several vertices and creases, as the implementation can be naturally carried out using a computer program. This is typically done by modeling origami using Denavit-Hartenberg-based analysis[15] that is widely used in the analysis of linkages. The connection between linkages and origami is very useful, especially for thick origami[16,17].

To ensure both sufficiency and necessity for rigid foldability, other detailed conditions (in addition to the Belcastro-Hull theorem[11,12]) must be carefully checked, such as the bird's feet condition on M/V assignment[18], which is both necessary and sufficient for a single vertex. Based on the rank deficiency of the kinematic Jacobian matrix (a linear expansion of the Belcastro-Hull theorem), a counting rule to calculate the generic DOF (degrees of freedom) of a finite origami pattern was also developed[13]. When the generic DOF is greater than zero, the corresponding pattern is rigidly foldable, otherwise no decisive conclusion can be drawn. The counting rule is given as follows:

$N_{GDOF} = N_{EO} - 3 - \sum_{k>3}(k-3)N_{Pk}$,

where N_{GDOF} denotes the generic number of DOFs, N_{EO} denotes the number of boundary edges of a pattern, k is the number of sides of a polygonal panel, and N_{Pk} denotes the number of *k-sided* polygons in an origami pattern. The derivation involves the Euler number of the manifold where the origami pattern lies on – the readers are encouraged to derive this formula by themselves. Based on the above condition, a pattern with only triangular panels is guaranteed to be rigidly foldable if it has more than 3 boundaries[6]. However, this condition is too strict practically. For example, many degree-4 origami patterns (patterns with only degree-4 vertices) are rigidly foldable, but they cannot be told by this formula. For degree-4 origami, case-by-case discussion is needed[19,20], and the panel angles and *M/V* assignment are both critical for rigid foldability (Figure 1H). Some ways to predict the folding behavior of rigid origami are to use mathematical tools like spherical trigonometry[4] or computational origami simulations[21].

It is important to realize that flat-foldability, developability, and rigid foldability are independent features of origami; having one feature does not imply the other (Figure 1J, Table 2). Different features

are suited for particular engineering applications. For example, robotic actuation requires a quick deployment of motion and release of energy, and hence non-rigid origami with multi-stability are often exploited for those purposes. On the other hand, sandwich composite cores require mass production and high stiffness, and hence developable rigid origami patterns are often used.

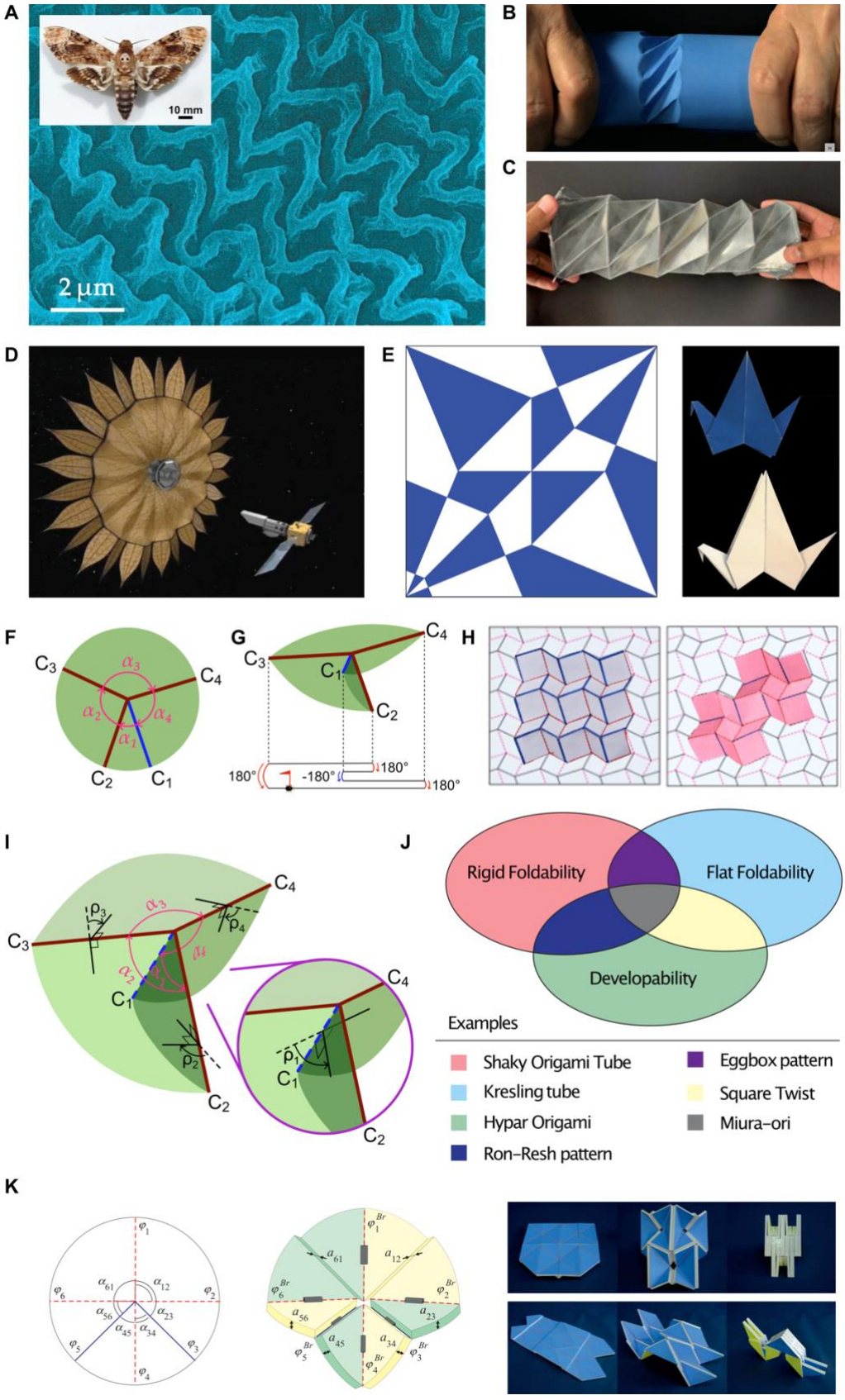

Figure 1: Origami overview. (A) Nature-inspired origami - Microscopical bellows pattern of the Giant Hawkmoth Achaerontia atropos shown in the inset (Credit: L.T. Wasserthal) [1]. (B) Spontaneous Kresling pattern obtained by twist buckling experiment. (C) Kresling pattern (Credit: S. Georgakopoulos). (D) The

unfolding of a starshade origami. Credit: NASA/JPL-Caltech [22]. (E) The crease pattern (left) of a Crane (right) using the 2-colorability (coloring) property. (F) A typical degree-4 origami vertex in its developed state. (G) The folded shape of a degree-4 vertex (below: flat-foldability condition). (H) Single crease layout with different mountain (thick-continuous blue lines) and valley (thin-dashed red lines). Left: square twist; right: Mars. Credit: Robert Lang's book [23]. (I) The turning angles between the panels of a degree-4 vertex used to apply the rigid foldability condition from Belcastro-Hull condition. (J) A Venn diagram (left) showing the relationship between flat foldability, developability, and rigid foldability, with typical examples given on the right. For a more complete list of patterns and their properties, please refer to Table 2. (K) Thick origami models. Thickness-accommodation of Waterbomb origami pattern using the offset hinge technique [16].

[H2] Thick origami models

Origami patterns are commonly crafted from thin sheets (approaching zero-thickness). To apply them to real engineering applications, thickness accommodation imposes additional constraints. In general, thick origami is treated on a case-by-case basis, and thus many methods exist to accommodate panel thickness[24]. By modeling thick origami using spherical linkages[17], the folding creases remain unchanged and the panels are either tapered[25] or offset[26] for a compact folding with least physical interference of panels. Such methods are only effective for one-dimensional folding and normally leave gaps or cannot be extended for patterns with large number of vertices considering two-dimensional folding. A kinematic approach has been proposed for rigid origami of thick panels – it involves replacing the spherical linkages with the spatial linkages at origami vertices consisting of four, five and six creases[16]. This is a comprehensive approach, which is capable of reproducing motions kinematically equivalent to those of zero-thickness origami (Figure 1K). Meanwhile, to achieve the thick-panel folding of the non-flat developable vertex, auxiliary panels as intermediate links are introduced to construct a plane-symmetric spatial linkage, which delivers compact folding[27]. Alternatively, a parallel-crease method can be used to create space for the panel thickness[28], however, this method introduces extra degrees of freedom as a four-crease vertex is transferred into an eight-bar linkage with at least two degrees of freedom. A recent contribution to the thick-panel origami consists of applying kirigami to the thick panels, whose advantage is to obtain the most compact folding of the Miura-ori patterns with uniform thickness[29]. Additional work has been done on the physical forms of crease lines, such as rolling-contact joints[30] or compliant joints, which results in the variable kinematic models for the folding process. As there are many methods to treat thick-panel origami, it is difficult to determine which is the most efficient method without considering the practical case of interest. For example, for large-scale deployable structures, the folding ratio and the stiffness take the highest priority, while for micro-scale structures, the fabrication and flexibility take the main role. Hence, other methods are expected in future developments.

[H2] Overview

From an engineering perspective, a few representative origami patterns are considered in this Primer, including the Miura pattern, the eggbox pattern, the waterbomb pattern, and the Kresling tube.

These representative patterns are used as examples for origami experiments and manufacturing with desired rigid or non-rigid behavior (see Experimentation section). In the Results section, geometric descriptions of origami structures are provided using the aforementioned patterns, and their geometric mechanics features are discussed. The unusual properties of origami structures have

enabled engineering applications across different fields ad scales, including sustainable and resilient buildings, mechanical metamaterials, robotics and medical devices (see Applications section). Basic information for testing origami, and standard formats to share origami designs, are recommended. The limitations and opportunities in the context of design and manufacturing of origami, and an outlook for the future of origami in engineering are envisioned.

Table 1: A sample of events regarding the evolution of origami engineering developments (not an exclusive list).

Year	**Key developments**
1950s	Origami notation – Yoshizawa-Randlett System[32]
1970	Discovery of Miura-ori for engineering applications[33]
1994	Origami mathematics[34–37] Origami in nature[38,39]
2002	Discovery of Kresling origami[2] Computational origami[21,40]
2005	Origami design by nature[1]
2010	Origami robotics[41,42]
2011	Thick origami[16,24,25]
2013	Geometric mechanics[37,43,44]
2014	Origami metamaterials[45,46]
2015	Origami multistability[47–49]
2016	Origami dynamics[50–52] Origami curvature[53,54]
2017	Structural analysis of non-rigid origami[55,56]
2019	Re-programmable metamaterials[43,57,58]
2020	Origami actuation[49,58,59]
2021	Modular origami[60]
2022	Experiments on geometric mechanics[46,61]

*Table 2: A sample of origami Patterns with featured properties, and applications (not an exclusive list). *Degree of Freedom.*

Patterns	**Featured Properties (incomplete list)**	**Engineering Applications**
Miura-ori	1-DOF*, Developability, Rigid Foldability, Flat Foldability, Auxeticity.	Space structures[62], Metamaterials[37], Frequency Selective Surfaces[63], Robotics[64]
Blockfold	1-DOF*, Developability, Rigid Foldability, Flat Foldability, Auxeticity.	Foldcore[65]
Eggbox	1-DOF, Rigid Foldability, Flat Foldability.	Sandwich structures[66], Metamaterials[37]
Waterbomb	Developability, Rigid Foldability, Flat Foldability.	Smart materials[67], Robotics (origami wheel)[68,69], Origami Stents[70]
Yoshimura	Developability, Rigid Foldability, Flat Foldability.	Folded concrete structures[71]
Kresling tube	Flat Foldability, Multistability.	Robotics[59,72], Impact mitigation[50]
Morph	1-DOF, Rigid Foldability, Flat Foldability, Reversible Auxeticity	Metamaterials[43,57]
Barreto-Mars[73]	1-DOF, Developability, Rigid Foldability, Flat Foldability, Auxeticity.	Solar cells
Flasher	1-DOF, Developability, Auxeticity.	Solar sails[74]
Ron-Resch	Developability, Rigid Foldability.	Energy absorption[75]
Miura-based tubes	1-DOF, Rigid Foldability, Flat Foldability.	Robotics[76]
Square twist	Developability, Flat Foldability, Auxeticity, Multistability.	Metamaterials[8], Programmable antennas[9]
Hypar origami	Developability, Multistability.	Metamaterials[4]
Origami Snapology	Rigid Foldability	Metamaterials[77], Waveguide[78]

Trimorph	1-DOF, Rigid Foldability, Flat Foldability, Reversible Auxeticity, Multistability.	Metamaterials[46]

[H1] Experimentation

This section presents experimental equipment and manufacturing techniques to create and test origami tessellations. Origami tessellations display fascinating mechanical properties, including tunable Poisson's ratio[37,43], multistability[46,58,72,79,80], tunable stiffness[81–84], and others, such as shape morphing[76,85,86], and acoustics[87,88]. The experimental evidence of such properties requires a careful sample manufacturing; and the design of *ad-hoc* experimental setups. The latter point is particularly important since the samples undergo large deformations simultaneously in longitudinal and transverse directions due to their intrinsic nonlinear folding mechanisms. Different laboratory equipment is required depending on the type of experiment to be performed, for example, qualitative or quantitative. In the latter case, loading frames, prototyping machines, cameras, transducers and acquisition systems are needed to test origami tessellations and to record, at the same time, experimental data. Below, the sequence of steps typically followed in fabricating and testing origami structures and metamaterials are discussed. Specifically, the manufacturing methods, folding and assembly, sample preparation and checks, experimental setups, and data collection and postprocessing are described.

[H2] Manufacturing methods

Origami tessellations have a long history[89]. They can be realized by different manufacturing techniques and base materials. Some of the most common materials and techniques are addressed below.

[H3] Paper and polymer-based models

The simplest way to create origami patterns is by folding craft paper (for example, Mi- Teintes, Canson), cardboard, polyester film (for example, Grafix Drafting Film), or composite film (e.g., Durilla Durable Premium Ice Card Stock)[59,82,90,91]. The folding lines can be marked or perforated with evenly spaced cuts. Laser cutters are used to perforate thin flat sheets along the folding lines, as shown in Figure 2A. Other electronic cutting machines (for example, Silhouette CAMEO, Silhouette America) can also be used to perforate thin sheets that can be folded using origami principles. The main advantage of paper-based origami is its easiness of realization. Furthermore, craft paper sheets have a very small thickness thus preventing panel thickness accommodation issues when extreme folding is achieved. Although very effective, this method can induce some difficulties in quantitative testing since the paper-based panels are very flexible. In fact, folding may not only be localized on the creases, but also in the panels through flexural deformation. This could lead to difficulty in the experimental validation of the underlying theory as the hypothesis of rigid foldability may not hold anymore.

[H3] Computer Numerical Control (CNC) milled models

A more effective method to create origami samples suitable for mechanical testing consists of assembling base components such as unit cell strips, panels, and hinges, which are cut by a CNC milling machine (such as the Roland MDX 540), as shown in Figure 2B[61]. The working principle of the milling machine concerns material removal through a rotating cutting tool driven by CAD/CAM (Computer Aided Design/Computer Aided Manufacturing) software. The base components can be made from different materials, such as polymeric (polycarbonate, polypropylene) or metallic (thin aluminum or steel sheets). The main advantage of this manufacturing method is its versatility and precision, which permits the realization of complicated shapes and multistable origami tessellations. In particular, this method allows fine-tuning of the energy landscape together with the mechanical properties of the tessellation, by varying crease thickness, panel geometry, and base material[46]. An attractive material to create zero energy creases (free rotating hinges) is Polypropylene since it guarantees excellent folding performance and fatigue resistance. On the other hand, if creases with specific rotational stiffness are required, they can be achieved by means of solid rubber (for example, silicon rubber)[46].

[H3] 3D printed models

Recent developments in additive manufacturing technologies have enabled the construction of intricate and complex topologies at different scale levels[92]. In this context, 3D printing represents an alternative method to creating origami samples, as shown in Figure 2C. The origami models are built layer by layer from a previously prepared 3D CAD file. Various materials and 3D printing technologies can be used depending on specific needs. For instance, origami tessellations have been realized by Fused Filament Fabrication[93,94], Material Jetting[95], Selective Laser Sintering[96], Stereolithography[97,98], Digital Light Processing[99,100] and, at the microscale, by two-photon polymerization laser lithography[101]. In addition, 4D printing adds the transformation over time (4th dimension) to 3D printing, which has been used to create multifunctional shape-morphing and self-foldable origami-based structures and materials[85,102–105]. The main benefit of additive manufacturing technique is its ability to make multi-material parts during a single printing step, thus avoiding complicated assemblage processes.

[H2] Folding and assembly

Once the manufacturing step is completed, one needs to fold along the creases and assemble the folded components to achieve the final origami structure. Developable patterns, such as the Miura-ori, can be realized by folding a single flat sheet of material along the crease lines. In contrast, non-developable patterns, such as the Eggbox, can be obtained through the folding and assembling of several sub-parts or pieces[61]. In the case of paper-based origami, the union among different parts is usually done using flaps and either double-sided tape or paper glue. On the contrary, assembled plastic models are realized by gluing several modular base components. Conveniently, each unit cell or component should have several seats and/or extensions to allow an easy assembly.

[H2] Sample preparation and checks

The quality and integrity of the sample is fundamental for the success of the experiments. Some discrepancies between theoretical prediction and experimental results are commonly related with sample defects such as aging, manufacturing, and fatigue issues. For instance, if a crease is broken or damaged, an imperfection is introduced into the tessellation, deeply influencing the experimental results. For such reasons, before executing any mechanical test on origami tessellations (for example, uniaxial testing), a careful visual sample check should be done in order to verify the integrity of the pattern and its actual dimensions at the rest configuration should be verified with measuring devices (tape measure and caliper) . In fact, the dimension of the sample at the rest configuration represents a common reference point for experiments, theory, and simulations[61]. Thus, it is an essential parameter when load vs displacement experimental data are compared with theoretical or numerical simulations (e.g., in MERLIN[54]) results.

[H2] Experimental setups

Origami tessellations are reconfigurable structures that exhibit simultaneous deformations both in the longitudinal and transverse directions. Further, origami systems can be highly stiff in certain directions and flexible in other directions[81]. Hence, different types of experimental apparatus and setups may be needed to investigate the behavior of origami structures depending on the nature of deformations and loading. Recently, the experimental setups to perform the uniaxial tests have been proposed to demonstrate the unique Poisson's ratio behavior of origami metamaterials[61]. In this work, it has been shown that the gripping mechanism, connecting the ends of the sample to the loading frame, plays a key role on the quality of the results obtained from the testing machine. The standard way to connect the sample to the loading frame is by clamping its ends to the machine, as shown in Figure 2D. Its drawback is that the gripping system prevents the free deployment of the pattern in the transverse direction, leading to non-uniform transverse deformation. This is evident by observing the shape assumed by the sample during tension and compression testing. In a tension test, the sample deforms into a dog bone shape; in compression, it deforms into a barrel shape. The proposed gripping mechanism[61] consists of a system of rail and sliders that allows proper attachment of the sample while permitting free transverse motion during the folding/unfolding process, as shown in Figure 2E.

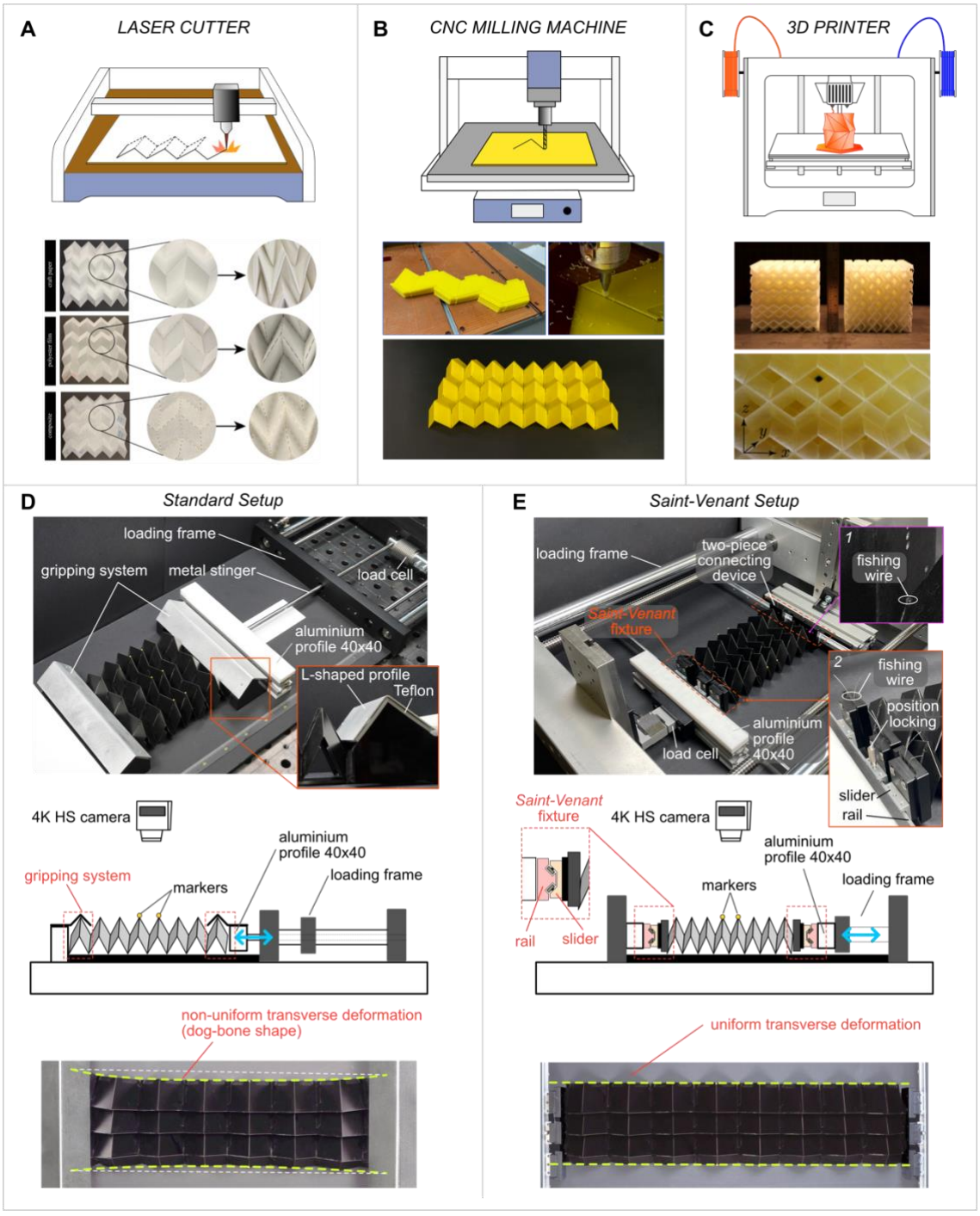

Figure 2: Origami experiments and manufacturing. (A-D) Different manufacturing techniques used to create origami tessellation. (A) Paper and polymer-based origami models via laser cutting [90], (B) CNC milled models realized using a milling machine [61], and (C) 3D printed models[98]. (D, E) Setups adopted to perform uniaxial testing on origami tessellation: (D) Standard setup and (E) Saint-Venant setup[61]. The Saint-Venant setup allows the sample to freely expand or contract in the transverse direction during folding and unfolding. This effectively prevents the sample from assuming a dog-bone-like shape and instead simulates the behavior of a periodic system during uniaxial testing.

Such a system, called a *Saint-Venant fixture*, eliminates Saint-Venant end effects during uniaxial testing experiments. This advanced setup permits a free deployment of the constrained sample, thus ensuring

that the origami tessellation remains truly periodic even when deformed in a tension or compression test. To obtain high resolution quantitative information from experiments, a loading frame machine is required for folding/unfolding the origami tessellation. The loading frame should be equipped with a load cell and a displacement transducer for recording the applied load as a function of the sample length. In order to reduce gravitational effects and avoid out-of-plane instabilities that could arise during the experiments, the whole experimental apparatus is arranged horizontally. Moreover, a Teflon plate should be placed underneath the sample to reduce friction and stick-slip phenomena. For the monitoring of the longitudinal and transverse deformation of the sample, a high-resolution camera must be placed orthogonally to the testing platform to record the experiments. This allows recording of the motion of a selected array of points, identified by colored markers, via digital imaging correlation (DIC) and tracking method. To facilitate the post-processing analysis via DIC, the color of the markers should be chosen to enhance the contrast with the tessellation.

[H2] Data collection and post-processing

The main data acquired during origami uniaxial testing are the load applied at one end of the sample, the length evolution of the sample, and the transversal and longitudinal deformation during the folding/unfolding process. A data acquisition system is often used to collect loads and displacements using a load cell and a displacement transducer. The acquisition system could be part of the loading frame used to perform the test or external to the testing machine. In the former case, the data acquisition is more straightforward but not as versatile as in the latter, where there are no limits on the number and type of transducers. In the case of an external acquisition system, it is common to use a cDaq (by National Instruments) or Arduino systems interfaced with a PC through software written either in LabVIEW or MATLAB/Simulink. The analysis of the experimental data (load/displacement) can be performed in a spreadsheet (such as Office Excel, LibreOffice Calc, IWork Numbers) or in an advanced software (such as Mathematica, MATLAB, or Python). A tailored experimental method is needed for monitoring the transversal and longitudinal deformation of the pattern together with the execution of the test. For this purpose, a DIC analysis and tracking method is essential for the frame-by-frame analysis of the recordings of the experiments and for estimating the motion of the markers previously located on the vertices of the pattern unit cell. Several strategies can be adopted to perform this analysis. The simplest way is manually analyzing a limited number of frames extracted from the recorded movie through open-source software (for example, VLC, Quick Time combined with Gimp, or NanoCad). If a frame-by-frame analysis of the movie is required, it can be performed by ImageJ filament open-source software or through in-house software written in Mathematica, MATLAB, or Python.

[H2] Actuation

The process of shape morphing in origami tessellations necessitates the utilization of external sources for actuation. The most commonly employed methods for actuating origami structures include pneumatic actuation and magnetic actuation. However, the emergence of 4D printing has introduced the possibility of using stimuli-responsive materials that can respond, for instance, to light or heat.

[H3] Fluidic actuation

Fluidic actuation of origami involves using pressurized air or gas to control and manipulate origami structures[93]. In this context, as the origami samples need to be inflated, they must be made impermeable to prevent air leakage. Typically, this is accomplished by coating origami structures with a thin layer of polydimethylsiloxane (PDMS) or by manufacturing them using plastic sheets with creases engraved onto them. To operate this method, the structure must be linked to an air supply system, such as a compressor or a simple air pump. This system allows for the regulation of both air pressure and flow rate. Since this actuation approach is tethered, the structure being activated needs to be equipped with an inlet for connecting the air source to the origami structure through flexible tubing.

[H3] Magnetic actuation

This method involves the utilization of magnetic fields to govern and manipulate origami structures, which are typically crafted from materials that respond to magnetic forces[106,107]. This is accomplished by integrating magnetic components into the origami structures, which are magnetized beforehand. Usually, these magnetic components are created by blending a silicone rubber precursor with specific proportioning of magnetic microparticles (NdFeB). Initially, the magnetic characteristics of these components must be gauged using a magnetometer. Subsequently, actuation is typically achieved using a 3D Helmholtz coil system capable of generating a uniform magnetic field, the direction and intensity of which can be altered by adjusting the current flowing through the coils. The primary advantages of this method are that it enables untethered and fast control of actuation.

[H1] Results

Typical properties exhibited by origami tessellations are characterized by "tunability" and "programmability". *Tunable* properties arise by virtue of the various folded states of the system and can be changed through the application of an active stimulus (e.g., force). The compliant folding of origami structures enables in situ control of the property they exhibit, making them excellent candidates for tunability. Several important mechanical properties like Poisson's ratio[37,43], elastic bandgaps[87,108], thermal expansion coefficients[109], and anisotropic stiffness[81,110] were previously studied and demonstrated to be tunable in origami metamaterials. Since the folding of origami is generally a smooth continuous process, the variation in the properties that are being tuned is also gradual. *Programmability*, on the other hand, refers to obtaining a property of interest based on variations in the design (e.g., geometry). This enables abrupt change in the properties of the origami tessellation with respect to the change in the programmability parameter[45]. Programmability parameters are typically associated with the geometric features of the panels or local defects that can be induced in the origami tessellations. In this section, the theoretical geometric results pertaining to kinematics of origami patterns, modeling frameworks of non-rigid origami, and some relevant properties (Poisson's ratio, wave dynamics, and multi-stability) are addressed.

[H2] Geometry of representative origami patterns

The configuration of an origami structure is characterized by its crease pattern as well as the dihedral angles between panels that define the folded state. The edges of the panels correspond to the folding-creases or boundaries of the structure, and the points of intersection of the creases are the vertices.

The configurational analysis of origami can be carried out using concepts of spherical trigonometry that enables us to find direct relations between the dihedral angles of the creases meeting at a vertex[23], and further determine the degrees of freedom of the vertex. The degrees of freedom of the entire origami structure, that may comprise several vertices, can be found using compatibility constraints imposed on the creases connecting adjacent vertices. Here we discuss the geometry of some widely used origami patterns.

[H3] The Miura-ori pattern

The Miura-ori pattern was originally designed for use in space applications such as deployable solar arrays[62,62]. The pattern can also be found in nature, in certain plant leaves[111]. The Miura-ori is a periodic two-dimensional tessellation (or lattice) with each unit cell having four parallelogram shaped panels as shown in Figure 3. The Miura-ori pattern is composed of degree-4 vertices where each vertex has either three mountain folds and one valley fold or vice versa (three valley folds and one mountain fold). The angle α denotes the smaller panel angle (Figure 3). When all the panels are rigid, it possesses a single degree of freedom. All the dihedral angles between adjacent panels depend on one single arbitrary folding angle, such as the crease-angle ϕ as shown in Figure 3. The crease-angle uniquely describes any partially folded state of the structure. In the fully developed state, all the dihedral angles are equal to π. In the completely flat-folded state, the dihedral angles are either 0 or 2π and structure is rigid. The relation between the two crease-angles (ϕ and ψ) of the Miura-ori is given by

$$\cos\left(\frac{\psi}{2}\right)\sin\left(\frac{\phi}{2}\right) = \cos\alpha$$

[H3] The eggbox pattern

The pattern takes the name from its appearance in the partially folded state. The eggbox is a two-dimensional tessellation formed with two types of degree-4 vertices which are non-developable. One of vertices has four mountain (or valley) creases. The other one has two mountains and two valley creases. The pattern has parallelogram-shaped panels arranged in a fully symmetric way as shown in Figure 3. When all the panels are rigid, the eggbox pattern deforms as a deployable single degree of freedom structure. The eggbox pattern exhibits a smooth folding from one flat-folded state, where two dihedral angles are 0 and the other two are π, to the other flat-folded state where the dihedral angles swap the values. Similar to the Miura-ori, the relation between the crease-angles (ϕ and ψ) of the eggbox is given by

$$\cos\left(\frac{\psi}{2}\right)\cos\left(\frac{\phi}{2}\right) = \cos\alpha$$

[H3] The Waterbomb pattern

The most widely studied waterbomb origami[112] comprises of degree-6 vertices, as shown in Figure 3. Depending on the tessellation, the degree-6 waterbomb unit cell can fold in different curved configurations. Figure 3 shows the tessellation of waterbomb unit cell with four mountain and two valley creases intersecting at a common vertex[113]. In general, the degree-6 waterbomb unit cell has three degrees of freedom. However, if the folding mode is restricted to be locally symmetric (four mountain creases with the same dihedral angle), then the configuration of the structure at any

partially folded state can be obtained from a single folding-angle chosen as an independent variable. The relation between the folding-angles ξ and γ is given by[114]

$$\tan\left(\frac{\xi}{2}\right) = -\frac{1}{\cos\alpha}\tan\left(\frac{\gamma}{2}\right)$$

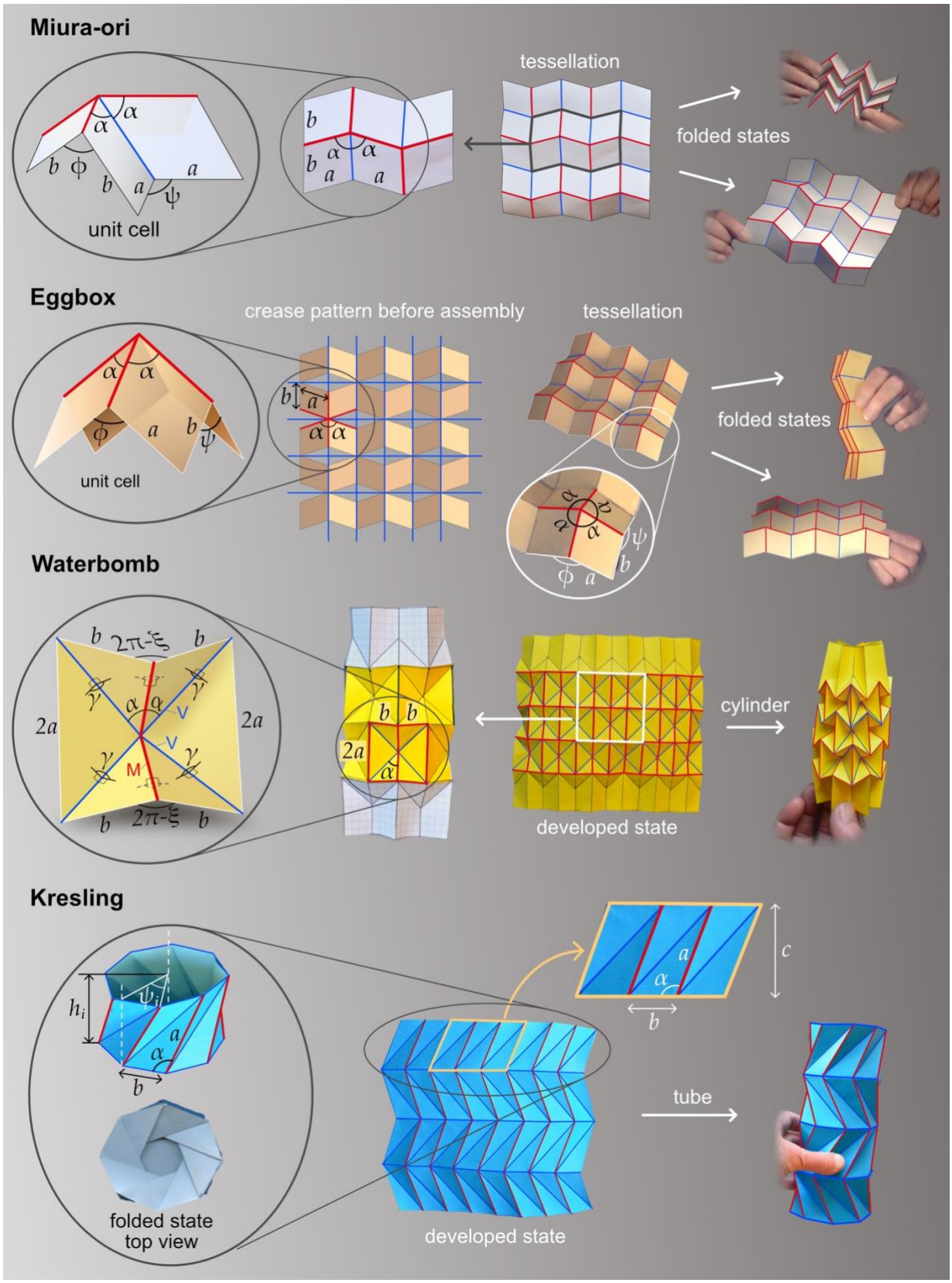

Figure 3: Schematic representation of the fusion of geometry, mathematics, and art through origami tessellations. The left column shows the unit cell, which forms the basis of the four tessellations considered here, with geometrical parameters dictating their mechanics and configurations. Labels "a" and "b" indicate the side lengths, "α" denotes the panel angle, and "ϕ", "ψ" and "ξ", "γ represent the crease angles and the folding

angles, respectively. ***Miura-ori.*** *From left to right: unit cell, unit module, tessellation in a deployed state, and two images showcasing different folded states of a physical Miura-ori tessellation.* ***Eggbox.*** *The non-developable nature of the pattern illustrated by its unit cell (left) requires that several strips cut from a flat sheet (middle-left) be assembled and glued together to obtain the desired tessellation (middle-right). On the right, two images showcase different folded states of a physical eggbox tessellation.* ***Waterbomb.*** *From left to right: Unit cell, unit module, crease pattern, and folded.* ***Kresling.*** *From left to right: perspective and folded state top views of an 8-sided polygon unit cell, one-piece crease pattern with reverse crease directions used to create the 4-story Kresling tube shown on the right. Label "h" indicates the height of the Kresling unit cell, while the subscript "i" in the parameters (h, ψ) takes on values 0 or 1 for the two stable states.*

[H3] The Kresling tube

The triangulated cylinder/tube of the Kresling pattern undergoes non-rigid folding. The tessellation is formed by connecting unit cells along one direction as shown in the Figure 3. The crease pattern of a single unit cell is shown in Figure 3 and is characterized independently by the parameters a, b, α, and n, where n represents the number of edges (or cells) in each unit cell. The parameter c is also defined as shown in the figure. The unit cell can exhibit bi-stability depending on its geometric parameters and materials. The two stable states of the unit cell are denoted as 0 and 1 and the corresponding folded configurations are characterized by the twist angles ψ_0 or ψ_1, respectively, and the unit cell heights h_0 or h_1, respectively. The two stable states are characterized by a geometric equivalence of the crease pattern parameters a, c, and α. Therefore, enforcing these parameters to be the same in the two stable states, they can be calculated[23] as follows,

$$\alpha = \cos^{-1}\left(\frac{x_0\left(x_0-\cot\left(\frac{\pi}{n}\right)\right)}{\sqrt{\left(x_0^2+1\right)\left[\left(\frac{h_0}{b}\right)^2\left(x_0^2+1\right)+x_0^2\csc^2\left(\frac{\pi}{n}\right)\right]}}\right),$$

$$a = b\sqrt{\left(\frac{h_0}{b}\right)^2+\frac{x_0^2\csc^2\left(\frac{\pi}{n}\right)}{x_0^2+1}},$$

$$c = \frac{b\sqrt{\left(\frac{h_0}{b}\right)^2\left(x_0^2+1\right)^2+x_0^3\cot\left(\frac{\pi}{n}\right)\left(x_0\cot\left(\frac{\pi}{n}\right)+2\right)+x_0^2}}{x_0^2+1},$$

$$x_{0,1} = 2\sin\left(\frac{\pi}{n}\right)\left[\frac{\sin\left(\frac{\pi}{n}\right)\sqrt{\cot^2\left(\frac{\pi}{n}\right)\csc^2\left(\frac{\pi}{n}\right)-\left[\tilde{h}\right]^2}-\cos\left(\frac{\pi}{n}\right)}{1\mp\tilde{h}+\left[1\pm\tilde{h}\right]\cos\left(\frac{2\pi}{n}\right)}\right],$$

with $\tilde{h} = (h_1/b)^2 - (h_0/b)^2$. The twisting angles for the two stable configurations are given by $\psi_0 = 2\tan^{-1}x_0$ and $\psi_1 = 2\tan^{-1}x_1$.

[H2] Structural analysis of origami

Some of the pioneering studies on origami structures focused on their rigid origami kinematics, which are of key interest for deployable structures and robotic applications. A few well-known software in this category includes: the Rigid Origami Simulator that runs a projection-correction algorithm for solving linearized compatibility equations [21], the GPU accelerated Origami Simulator [191], and the Rhino plug-in Crane [https://dl.acm.org/doi/full/10.1145/3576856].

However, in the last decade, interest in the use of origami for mechanical and civil engineering applications such as energy absorption, vibration control, and load-bearing have gained prominence. Investigation of origami for such applications requires modeling the non-rigid behavior of origami and carrying out structural analysis simulations. Besides shell-based Finite Element Analysis, structural analysis of origami is typically carried out using an efficient Reduced Order Model called *bar-and-hinge model*, formally introduced by Schenk and Guest [55], which captures the folding deformations, bending of panels, and in-plane stretching of panels. In this model, the panels are replaced by bars that are placed along all the creases of the origami pattern as well as the panel diagonals. The stiffness associated with folding and panel bending is modeled through rotational springs or hinges between the triangulated truss-type panels. Some of the first bar and hinge models[55] were formulated to capture small deformations of origami tessellations during structural analysis. Later on, improvements were made to bar and hinge models to capture various features like isotropic panel stretching[81], complex panel-bending deformations and large non-linear deformations[54]. For example, Figure 4A shows bending of an eggbox tessellation using the MERLIN software that implements a nonlinear mechanics formulation associated with the bar-and-hinge model[54]. Figure 4B shows representative simulation results by MERLIN, obtained from uniaxial tension test of origami tessellations, that show good agreement with experimental data.

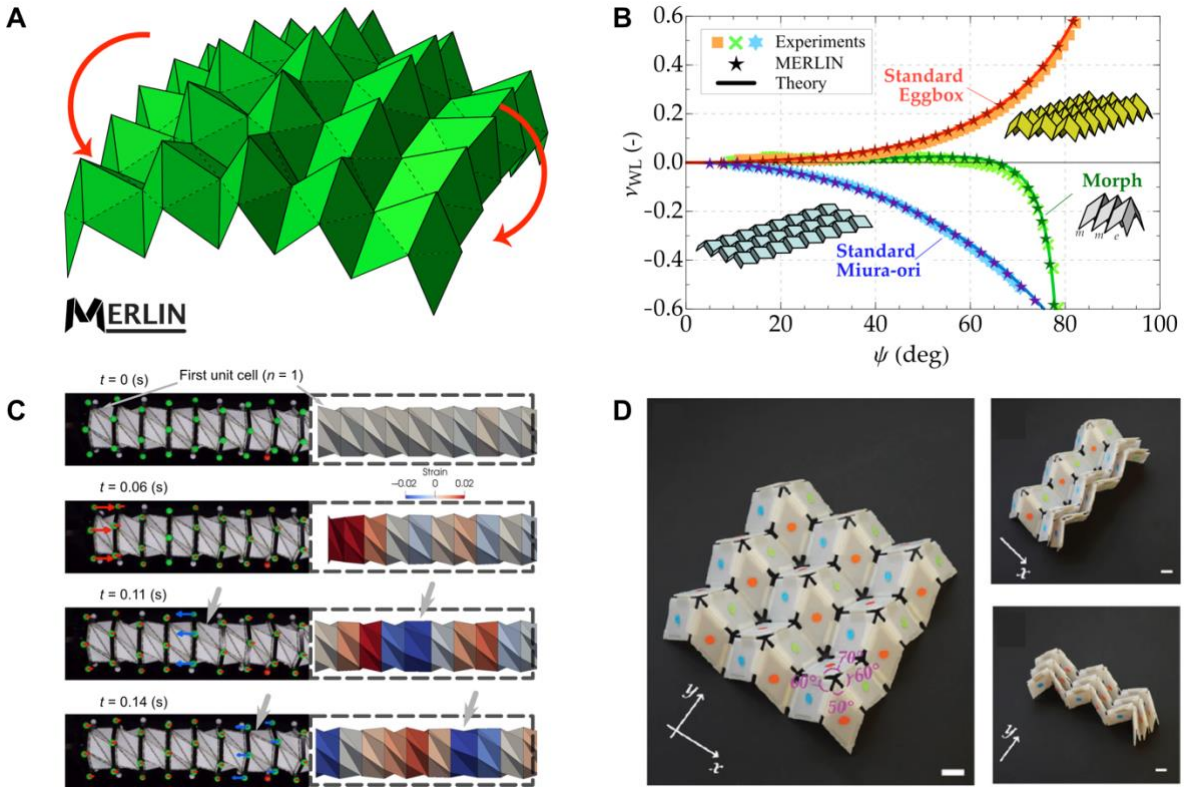

Figure 4: Mechanics of origami structures. (A) The MERLIN software for structural analysis of origami. (B) Poisson's ratio results of the Miura-ori, eggbox, and morph origami metamaterials from theory, experiments (all the experiments use 3x7 units), and MERLIN simulations[61]. The Poisson's ratio variation for the Miura-ori is negative, and for the eggbox is positive. The morph pattern is composed of 7 layers, each having 2 units and the Miura-ori mode and 1 in the eggbox mode (see inset), exhibits a Poisson's ratio switch from positive to negative. (C) Wave propagation in the Kresling tube origami (image adopted from ref. [88]). (D) Different multi-stable states of the Trimorph origami (image adopted from ref.[46]).

[H2] Poisson's ratio

Poisson's ratio is an important property that dictates the deformation of materials. The magnitude of Poisson's ratio of linear elastic isotropic materials is restricted within a small range from -1 to +0.5. Interestingly, origami metamaterials can exhibit Poisson effects that vary significantly with the folded geometry of the structure[37], and beyond the conventional range as they are typically not isotropic. For example, Miura-ori pattern can exhibit in-plane Poisson's ratio values all the way from negative infinity to zero achieving the extreme values when it is in a developed state or the flat-folded state. The negative Poisson effect in Miura-ori makes it an auxetic metamaterial. On the other hand, the Eggbox pattern displays tunable in-plane Poisson's ratio values from zero to positive infinity as it folds from one flat-folded state to the other flat-folded state. The Poisson's ratio results for Miura-ori and eggbox origami metamaterials are shown in Figure 4B, where good agreement between theory and experiments are obtained. Recently, novel origami patterns were discovered, namely Morph[43] (see Figure 4B) and Trimorph[46], which can exhibit any real value of Poisson's ratio (negative infinity to positive infinity) depending on their folded configuration. Origami metamaterials exhibit a wide variation in the value of Poisson's ratio as they are being folded or deformed. However, recent

research has shown that it is also possible to design origami patterns in such a way that the Poisson's ratio value is held nearly constant under large deformations[115]. All these results indicate the capability of origami metamaterials to be programmed or tuned to display desired Poisson effects.

[H2] Wave dynamics

Origami metamaterials have two major features that are useful for applications related to wave-propagation and vibrations. Firstly, the high contrasting levels of stiffness in the system in terms of crease folding, panel bending, and panel stretching can lead to elastic bandgaps, which are frequency ranges with no wave-propagation. Secondly, the frequency range of the bandgaps and other related characteristics can be easily tuned by compliant folding of origami. A mathematical technique called Bloch wave reduction can be employed to carry out wave propagation studies in periodic media such as origami tessellations[87]. While typical calculations to study dynamics of tessellated structures could involve considering several unit cells, the Bloch wave approach reduces the calculation effort to a single cell within the periodic system by virtue of its translational symmetry. Unlike several lattice structures, where the structural interactions are restricted to the nearest neighbouring nodes of a unit cell, origami metamaterials may exhibit nonlocal structural behaviour as noted in previous research[87]. Hence, the application of Bloch boundary conditions should be careful enough to ensure that such (beyond nearest neighbour) nodal interactions are taken into account for accurate prediction of dynamic properties. Using such an approach, researchers have studied wave dynamics and bandgap structures in origami metamaterials. For example, modal characteristics of standard Miura-ori and Eggbox patterns revealed the presence of elastic bandgaps that are tunable by virtue of their folded configuration and programmable by virtue of their panel geometry[87]. That is, the frequency ranges of the bandgaps obtained could be controlled (in theory) by subjecting the origami tessellation to folding, or by re-designing it to have different panel sizes or angles. In another study on wave dynamics, one-dimensional origami-based lattice structures with triangulated cylinders were designed and experimentally found to exhibit rarefaction waves for applications in impact mitigation[88], as shown in Figure 4C. There are two aspects that influence the tunable dynamic properties of origami lattice structures. One is the tunable geometry of the system by virtue of folding. The other is the mass and stiffness of panels and hinges. The former aspect is typically independent of the base material with which the origami structure is made of. The latter aspect depends on the material used and therefore influences the natural frequency ranges and to some extent the modal characteristics. Hence, the material should be chosen based on the target frequencies relevant to the engineering application. However, it is expected that the tunability of the dynamic properties can be achieved irrespective of the choice of base material.

[H2] Multi-stability

Some origami structures experience multiple stable states such that each of them locks a particular configuration. These structures with multiple stable states can serve as basic unit cell for architected materials, creating properties that differ from those of traditional materials. For example, the snap-through action (i.e., the deformation process between different stable states) of the Kresling origami can be activated by non-contact forces, such as those generated by magnetic fields[59]. In addition, the

multi-stable origami concept can be used to create a tessellation with switchable mechanical properties: the Trimorph pattern made of a tessellation of tristable origami unit cells, can switch between different metastable phases to produce distinct stiffness, anisotropy, and Poisson's ratio, as shown in Figure 4D[46].

Conceptually, the multi-stability in origami structures usually comes from two types of incompatibility. The first type is the incompatibility between the stress-free states of the folding hinges between the origami panels. This happens when the zero energy, or stress-free, state of the folding hinges of an origami are not compatible with its rigid folding kinematics, such that the folding hinges can never be all stress-free at the same time[116]. The second type is the incompatible panel geometries that forbid rigid folding, such as the square twist, Kresling pattern, and many others[10,45,48,59,80,88]. Overcoming rigid foldability requires bending and stretching of the panels, which creates energy barriers between stable states where panels are usually flat and unstretched. Both types of incompatibility could be present in one pattern, at the same time, such as in the Trimorph pattern, in which the "line defect" is caused by the first source, while the "point defect" is caused by the second source[46].

[H1] Applications

Due to the inherent cross-disciplinary nature of its design principles, origami is a rich source of inspiration for creating cutting-edge materials and structures with a broad range of applications. A non-exhaustive list includes applications in engineering[14], physics[43], material science[37], microrobotics[117], waveguiding[118], impact mitigation[88], space structures[22], solar technologies[119], and artificial muscles[120]. Some distinguishing characteristics of origami are scalability and high deployability[51,117,121,122]. The former broadens the spectrum of applications across multiple length scales as the behavior of origami structures is primarily governed by geometry in several cases. The latter allows achieving extremely reconfigurable shapes and tunable mechanical properties in static and dynamic regimes. Thus, origami principles can inspire design of materials and structures with myriad applications[120,123–125]. Broad engineering areas of application that were inspired by origami in recent years are discussed below. Specifically, origami has generated ideas for futuristic infrastructure development, has inspired the creation of several artificial materials concepts, including metamaterials, has been used to create soft robots and medical devices, and has enabled efficient transport of large structures in space applications. It is to be noted that the application areas discussed below are not mutually exclusive. Applications towards one topic (e.g., mechanical metamaterials or soft robotics) can have relevance to applications related to another topic (e.g., infrastructure or medical devices).

[H2] Sustainable and resilient infrastructure

Novel origami-based mechanisms have been implemented in architecture to create responsive building skins and adaptive diagrid façades capable of maximizing solar shading, acoustic performance, energy efficiency, and structural performance[119,126]. Usually, the energy efficiency interventions on buildings, such as wall insulation, once put in place, remain fixed over time regardless of the climatic conditions. On the contrary, the use of kinetic origami-based building skins can lead to maximizing energy efficiency at all hours of the day, optimizing the relation between internal comfort

and exterior climate conditions. For example, some studies showed that kinetic origami-based facades optimize daylight by approximately 50% from March to September and about 30% from October to February, compared to the case of static façades, thus improving indoor visual and thermal comfort[127,128]. Another example is the futuristic shape-adaptive shading origami-based system installed on the facades of the *Al Bahar Towers*, located at the financial center of Abu Dhabi[129,130]. The motile façade installed on these towers reduces the internal temperature by 50% with a substantial decrease in energy consumption for air conditioning and diminishing CO2 emissions by 1,750 tons per year[131]. Furthermore, origami-based systems are starting to be used to create kinetic solar arrays capable of tracking sun motion and, thus, maximizing solar energy intake[132,133].

Origami principles of reconfigurability and deployability can offer a valuable contribution to creating robust and resilient buildings potentially minimizing material usage, thus leading to a dramatic reduction of embodied CO2 emission[128,134,135]. In this context, there have been several efforts by researchers to obtain large-scale deployable structures inspired by origami behavior. For example, pneumatic and multistable origami structures have been shown to allow the design of large-scale structures that can be deployed from a very compact configuration, as shown in Figure 5A (top)[58]. Another example involves lightweight canopy structures that can be realized by coupling and stacking of origami tubes in different directions, as shown Figure 5A (middle)[81]. This leads to deployable roofs with high out-of-plane stiffness. Other researchers used modified geometries to create novel accordion-type shelters with improved structural stability and stiffness, as shown in Figure 5A (bottom)[136].

[H2] Mechanical metamaterials

Metamaterials are artificial materials that can exhibit exotic properties superior to those of constituent materials[137]. Mechanical metamaterials are a sub-class of metamaterials where the properties of interest are mechanical in nature, such as acoustic, thermal, or elastic. Typically, metamaterials are obtained by repeating a unit cell whose geometry is designed once and for all and cannot vary over time. Contrastingly, origami can transform its geometry continuously from a folded to an unfolded configuration, thus widening the design space. While the discussion on metamaterials in the previous sections focused on aspects of modelling, analyzing, or understanding the behavior of origami structures in general, here, we present the broad range of contexts within which origami concepts were applied to create mechanical metamaterials. Since metamaterial properties are strictly related to the unit cell geometry, origami permits achieving extremely tunable and reprogrammable mechanical properties[138–140]. Moreover, the relationship between stiffness of the panels and the creases provides opportunities to design the energy landscape of the resultant metamaterials[141–143]. This is useful to attain multistability, self-deployment, or mechanical computing systems[144]. Origami design principles have also been successfully applied to conceive origami-based metamaterials exhibiting auxetic behavior[37,145,146], tunable Poisson's ratio[80,82], self-locking[147,148], high strength-to-weight ratio[69,149], and tunable stiffness[83,143,150,151]. Some researchers have shown that, by properly designing kinematic paths, it is possible to achieve lockable and flat-foldable modes[57,82] (see Figure 5B). In addition to extreme static mechanical properties, origami-based metamaterials permit the

achievement of tunable dynamic properties. For instance, the morphing of the origami tessellation leads to controlling electromagnetic or elastic waves[152,153], deflecting light[154], and opening and widening bandgaps[87,118,155–157]. Origami metamaterials can also exhibit interesting coupling behaviors that are not typically observed in conventional materials, such as shear-normal coupling[46] and compression-twist coupling effects[158].

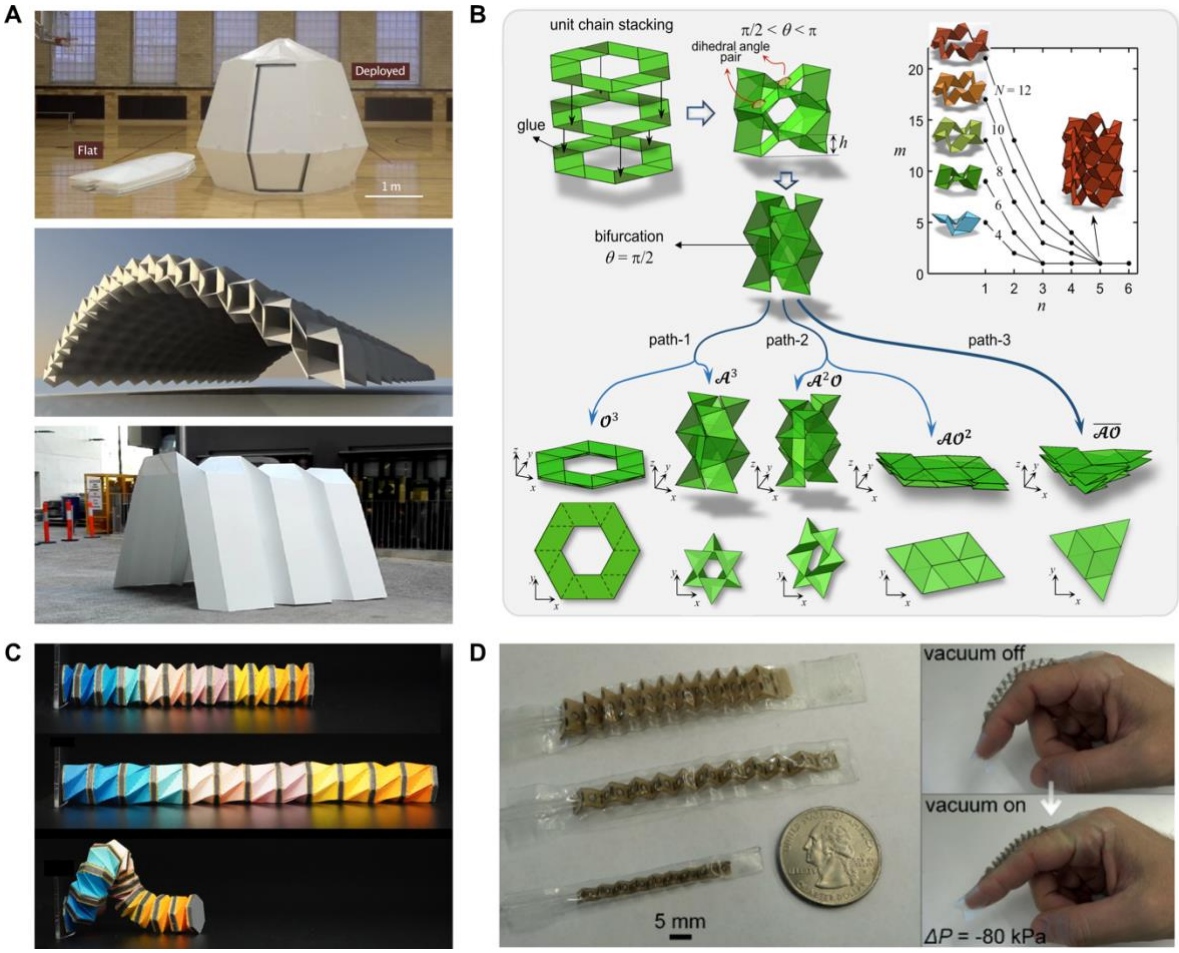

Figure 5: Origami applications. (A) Examples of origami-based canopies and shelters[58,81,136]. (B) Multiple kinematic paths leading to lockable and flat-foldable modes in 3D origami-inspired metamaterials[82]. (C) Omnidirectional origami robot arm obtained by assembling several Kresling basic units, controlled via magnetic actuation[159]. (D) Miniature fluid-driven origami-inspired artificial muscle[120].

[H2] Soft robotics

In recent years, origami has been a source of inspiration for several applications in robotics. Soft robotics applications require gradual changes in stiffness and significant reconfigurability. Origami structures are well known to exhibit multistability, tunable stiffness, and shape morphing and hence, can meet the design requirements for soft robotics. Exploiting origami-based design principles, robotic arms have been realized through the uniaxial repetition of Kresling unit cells capable of multidirectional morphing, grasping objects, and exploring hard-to-reach areas via magnetic actuation, as shown in Figure 5C[59,106,159,160]. Within this framework, origami morphing capabilities allow

the realization of grippers[161], artificial hands that gently grasp fragile objects without breaking them[162–164]. Origami design principles can also be a source of inspiration to create programmable artificial muscles with multidimensional actuation[120]. Origami robots capable of crawling, jumping, and swimming[93,159] indicate the potential for advanced applications in this field.

[H2] Medical devices

The progress in rapid prototyping technology and the rising demand for increasingly miniaturized tools fostered the implementation of origami design in the biomedical industry for *in vivo* or *ex vivo* purposes. The scalability, high deployability, and extreme packaging capabilities of origami make them particularly suitable for minimally invasive medical devices[165,166]. The auxetic nature of several origami patterns permits the conception of novel surgical tools that can access the human body through a small incision, travel in a very compact state to the intervention destination and deploy in their functional shape to execute the surgery. Origami designs have been explored for facilitating the execution of biopsy[167], MRI-guided radiofrequency ablation (RFA) and catheter insertion[168], or inspection of hard-to-reach sites[169]. Origami-based deployable surgical reactors have been designed for potential use in face-lift operations[170] and adopted to create novel orthopedic implants[171,172], and tissue scaffolds[173,174]. Origami-based self-folding microrobots have been realized to enable encapsulation, gastrointestinal microsurgeries[175], and drug delivery[176]. Origami-based structures have been conceived to assist retinal microsurgery[121,177] and as a support system for optimizing the insertion of flexible instruments in robot-assisted procedures (RAS)[178]. Within this framework, origami-based microgrippers have been designed for the capture and retrieval of objects and biopsies[179,180], minimizing invasiveness and potential human errors.

[H2] Space technology

Space structures, such as solar arrays or satellites are large scale structures that need to be compactly transported and deployed in the target orbits. Efficient transport of such structures requires them to be of light weight and to be folded into a small volume. Origami patterns can be implemented in the design of extremely lightweight, densely packed membranes and other devices to be deployed, once placed at target locations in space. Deployable membranes can serve as solar sails, propelled by the solar wind, for exploration missions; as solar power arrays for satellites, for solar energy collection, conversion and transmission; as reflectarray antennas; space telescopes; and for protective shields[181,182]. The Miura-ori pattern was a key invention that enabled compaction and deployment of space structures[33,62,183,184]. Designs of origami-based solar sails have evolved over years, for example, with a different deployment technique which uses radial segments, wrapped in spirals around a central hub, that unfold tangentially[185]. The pattern resembles a moonflower just after opening, and is nicknamed "origami flasher"[22,133,186,187]. Another variant, a 4-quadrant square solar sail is extended in the diagonals by telescopic booms. The recent Kresling pattern[1,2,188,189], allows cylinders to be actively folded and unfolded, like bellows, and is applied to the Sunshield project of the IXO-Space

Telescope[190], the Mars Rover drill protection, and for Origami Antennas of Space-ground communication[116].

[H1] Reproducibility and data deposition

[H2] Reproduction of Samples

Physical samples of origami are made with various methods. In general, the kinematics of origami structures is primarily driven by its geometry and is less sensitive to the materials being used, which is one of the many virtues of origami designs. However, deviations in the geometric structure, such as misalignment in the crease pattern, could lead to significant discrepancy from expected behavior. In a previous study, experiments and numerical simulations have shown that geometric imperfections could hinder the foldability of origami structures and increase its compressive stiffness[90]. This effect is less significant when the origami is made with compliant (or soft) materials but becomes severe for rigid materials. For Miura-ori, the square residual of the Kawasaki-Justin condition (i.e., Kawasaki excess), correlates approximately linearly with the increase of stiffness of imperfect Miura-ori structures[90]. Small geometric imperfections stiffen the originally programmed mode but generally do not alter the mode shape.

Data Deposition. Origami structures are usually shared in data formats that store meshes, which must include at least two pieces of information: the coordinates of the vertices (or nodes); the groups of vertices that belong to each face (or panel). A typical example of such format is the OBJ format, which is supported by the Rigid Origami Simulator[191], the Origamizer[192], and MERLIN[54]. Although STL format is the most used one for 3D printing and animation editing, it is not suitable for origami because all faces in STL must be triangular, while polygonal faces are common in origami designs. Recently, researchers formulated the FOLD (Flexible Origami List Datastructure) format that is dedicated to origami design, with an extension ".fold"[193]. Compared to the standard industrial formats, the FOLD format not only stores the static information of an origami design, but also allows "frames" to be collected that depict the folding process of an origami. For flat-folded origami, the FOLD format includes the topological stacking order of faces that overlap geometrically to distinguish different folded states. The FOLD format is gradually becoming popular among the origami community. Origami Simulator[20] and MERLIN[54] support the FOLD format. Note that all formats mentioned above apply to both partially folded origami and its flat crease pattern.

[H1] Limitations and optimizations

Most current developments in origami engineering are based on adaptation of some existing origami patterns to certain applications or are those that gained attention by serendipitous discovery. First principles-based systematic design of new origami patterns that can exhibit exotic engineering properties is a challenging problem. Although there have been developments in the recent years towards inverse design of origami for engineering applications, they are still in rudimentary stages. The theoretical or numerical design of origami patterns for target requirements is an active area of research[194–196] and more developments are needed in this direction, to make origami engineering versatile across applications. The challenges arise from two contexts – one is related to the choice of

design variable space and the other is related to the choice of engineering properties that are explored. Further, in most cases, the designs must satisfy requirements related to developability, flat-foldability, or rigid folding, which significantly constraints the solution space. In terms of applications, design of crease hinges, especially in the context of thick origami is not systematically investigated and hinders large scale and reliable use of origami structures made from thick sheets of material or thick panel prisms.

Behavior of origami patterns is significantly influenced by the presence of imperfections in their geometry. Most studies on origami patterns demonstrate the results through prototypes made from regular symmetric structures with no imperfections. However, presence of geometric imperfections in the patterns can lead to unexpected behavior. Hence, extensive studies by incorporating imperfections due to manufacturing defects should be performed while investigating the suitability of origami for applications.

Limitations of efficient manufacturability of origami structures also exist, especially in the context of non-developable patterns. Most current methods involve manual assembling of individual modules to form the final tessellated structure. Further, in the context of developable patterns, the tessellated structures need manual folding through creases marked on the entire sheet. Advanced manufacturing techniques such as 3D printing can be investigated to seek potential alternatives to these limitations.

Exploring microscale sample experimentation remains a relatively unexplored territory demanding further investigation. While origami structures are believed to exhibit scale-independent mechanical properties, suggesting that larger-scale experiments should replicate the mechanical behavior of microscale origami, the process of miniaturizing origami to this level introduces significant complexities due to the changing underlying physics governing the mechanical response at different scales. These complexities encompass various factors, including the substantial impact of Van der Waals forces on the mechanical response of microscaled origami, the intricate challenges associated with manufacturing due to limited materials and manufacturing technologies capable of achieving nanometer precision, as well as the development of miniature testing platforms.

Origami structures can be highly kinematic in nature with multiple degrees of freedom. Through analysis of the structure's mobility should be carried out before adapting origami for applications. If unwanted modes of mobility are found to exist, appropriate constraints should be applied on the structure to lock or guide it into desired configurations.

[H1] Outlook

While origami science is a more mature field, origami engineering has the potential to revolutionize the fields of engineering and design by enabling the creation of complex, lightweight, and adaptable structures across scales, which can be manipulated and deployed in various applications. Beyond modeling and manufacturing of origami, automated folding and actuation can lead to major advances

especially with multi-physics considerations (for example, magnetic actuation[59,197]). Thus, origami engineering has potential for continued advances in several fields ranging from robotics, space structures, architecture, and medical technology. The latter field holds great potential, especially as medical Doctors and Engineers collaborate in a true interdisciplinary fashion including actual experiments in animals with potential for further findings in humans. Modeling of an origami structure is problem specific and therefore, a single framework may not be readily applicable. Therefore, researchers have adopted context specific modeling approaches for origami. As origami ideas permeate different fields, several origami modeling frameworks and packages are expected to be developed in the future. Alongside, one could expect a variety of design approaches to also be developed. The material used to make the origami may play a key role and challenge the development of manufacturing processes for origami-based structures. While many recent studies on origami use paper-based models to demonstrate ideas, real applications, depending on the length scale of interest, could use a variety of materials ranging from polymeric-materials at micron scale[101] and construction materials like steel or concrete[71] that could help reshaping our infrastructure toward more sustainable solutions. Another fascinating material to be explored are biological materials and living tissues, which could revolutionize the medical field[198].

References

1. Kresling, B. Origami-structures in nature: lessons in designing “smart” materials. *MRS Online Proc. Libr. OPL* **1420,** (2012).

2. Kresling, B. Folded tubes as compared to kikko (‘tortoise-shell’) bamboo. *Origami* **3,** 197 (2002).

3. Foster, C. G. Some Observations on the Yoshimura Buckle Pattern for Thin-Walled Cylinders. *J. Appl. Mech.* **46,** 377–380 (1979).

4. Liu, K., Tachi, T. & Paulino, G. H. Invariant and smooth limit of discrete geometry folded from bistable origami leading to multistable metasurfaces. *Nat. Commun.* **10,** 4238 (2019).

5. Hull, T. *Project origami: activities for exploring mathematics*. (CRC Press, 2012).

6. O’Rourke, J. *How to fold it: the mathematics of linkages, origami, and polyhedra*. (Cambridge University Press, 2011).

7. Demaine, Erik D., and Joseph O’Rourke. *Geometric folding algorithms: linkages, origami, polyhedra.* (Cambridge university press., 2007).

8. Ma, J., Zang, S., Feng, H., Chen, Y. & You, Z. Theoretical characterization of a non-rigid-foldable square-twist origami for property programmability. *Int. J. Mech. Sci.* **189,** 105981 (2021).

9. Wang, L.-C., Song, W.-L., Zhang, Y.-J., Qu, M.-J., Zhao, Z., Chen, M., Yang, Y., Chen, H. & Fang, D. Active Reconfigurable Tristable Square-Twist Origami. *Adv. Funct. Mater.* **30,** 1909087 (2020).

10. Li, Y. & Pellegrino, S. A Theory for the Design of Multi-Stable Morphing Structures. *J. Mech. Phys. Solids* **136,** 103772 (2020).

11. Belcastro, S.-M. & Hull, T. C. Modelling the folding of paper into three dimensions using affine

transformations. *Linear Algebra Its Appl.* **348,** 273–282 (2002).

12. Hull, T. C. *Origametry: Mathematical methods in paper folding*. (Cambridge University Press, 2020).

13. Tachi, T. Geometric considerations for the design of rigid origami structures. in *Proc. Int. Assoc. Shell Spat. Struct. IASS Symp.* **12,** 458–460 (Elsevier Ltd Shanghai, China, 2010).

14. Peraza Hernandez, E. A., Hartl, D. J. & Lagoudas, D. C. Active origami: modeling, design, and applications. (2018).

15. J. Denavit, R. S. H. A Kinematic Notation for Lower-Pair Mechanisms Based on Matrices. *J. Appl. Mech.* 215–221 (1955). doi:10.1115/1.4011245

16. Chen, Y., Peng, R. & You, Z. Origami of thick panels. *Science* **349,** 396–400 (2015).

17. Chen, Z. Y., Yan. *Motion Structures: Deployable Structural Assemblies of Mechanisms*. (CRC Press, 2011).

18. Abel, Z., Cantarella, J., Demaine, E. D., Eppstein, D., Hull, T. C., Ku, J. S., Lang, R. J. & Tachi, T. Rigid origami vertices: conditions and forcing sets. *J. Comput. Geom.* **7,** 171–184 (2016).

19. He, Z. & Guest, S. D. On rigid origami I: piecewise-planar paper with straight-line creases. *Proc. R. Soc. Math. Phys. Eng. Sci.* **475,** 20190215 (2019).

20. He, Z. & Guest, S. D. On rigid origami II: quadrilateral creased papers. *Proc. R. Soc. Math. Phys. Eng. Sci.* **476,** 20200020 (2020).

21. Tachi, Tomohiro. Simulation of Rigid Origami. in *Origami 4 Fourth Int. Meet. Origami Sci. Math. Educ. 1* 175–187 (2009).

22. Space-origami: make your own Starshade Jet Propulsion Laboratory, Caltech. *NASAJPL Edu* at <https://www.jpl.nasa.gov/edu/learn/project/space-origami-make-your-own-starshade/>

23. Lang, R. J. *Twists, tilings, and tessellations: Mathematical methods for geometric origami*. (CRC Press, 2017).

24. Lang, R. J., Tolman, K. A., Crampton, E. B., Magleby, S. P. & Howell, L. L. A Review of Thickness-Accommodation Techniques in Origami-Inspired Engineering. *Appl. Mech. Rev.* **70,** (2018).

25. Tachi, T. Rigid-foldable thick origami. *Origami* **5,** 253–264 (2011).

26. Edmondson, B. J., Lang, R. J., Magleby, S. P. & Howell, L. L. An Offset Panel Technique for Thick Rigidily Foldable Origami. in (American Society of Mechanical Engineers Digital Collection, 2015). doi:10.1115/DETC2014-35606

27. Gu, Y., Wei, G. & Chen, Y. Thick-panel Origami Cube. *Mech. Mach. Theory* **164,** 104411 (2021).

28. Ku, J. S. & Demaine, E. D. Folding Flat Crease Patterns With Thick Materials. *J. Mech. Robot.* **8,** (2016).

29. Yang, J., Zhang, X., Chen, Y. & You, Z. Folding arrays of uniform-thickness panels to compact bundles with a single degree of freedom. *Proc. R. Soc. Math. Phys. Eng. Sci.* **478,** 20220043 (2022).

30. Lang, R. J., Nelson, T., Magleby, S. & Howell, L. Thick rigidly foldable origami mechanisms based on synchronized offset rolling contact elements. *J. Mech. Robot.* **9,** 021013 (2017).

31. Pehrson, N. A., Magleby, S. P., Lang, R. J. & Howell, L. L. Introduction of monolithic origami with thick-sheet materials. *Proc. IASS Annu. Symp.* **2016,** 1–10 (2016).

32. Yoshizawa, A. *Akira Yoshizawa, Japan's Greatest Origami Master: Featuring over 60 Models and 1000 Diagrams by the Master*. (Tuttle Publishing, 2016).

33. Miura, K. *Zeta-Core Sandwich- Its Concept and Realization*. (Institute of Space and Aeronautical Science, University of Tokyo, 1972).

34. Hull, T. On the mathematics of flat origamis. *Congr. Numerantium* 215–224 (1994).

35. Lang, R. J. Mathematical algorithms for origami design. *Symmetry Cult. Sci.* **5,** 115–152 (1994).

36. Guest, S. D. & Pellegrino, S. The Folding of Triangulated Cylinders, Part I: Geometric Considerations. *J. Appl. Mech.* **61,** 773–777 (1994).

37. Schenk, M. & Guest, S. D. Geometry of Miura-folded metamaterials. *Proc. Natl. Acad. Sci.* **110,** 3276–3281 (2013).

38. Saito, K., Nomura, S., Yamamoto, S., Niiyama, R. & Okabe, Y. Investigation of hindwing folding in ladybird beetles by artificial elytron transplantation and microcomputed tomography. *Proc. Natl. Acad. Sci.* **114,** 5624–5628 (2017).

39. Kresling, B. Folded and unfolded nature. in *Origami Sci. Art Second Int. Meet. Origami Sci. Sci. Origami Otsu Jpn.* 93–108 (1994).

40. Demaine, E. D. & Demaine, M. L. Recent results in computational origami. in *Origami3 Third Int. Meet. Origami Sci. Math. Educ.* 3–16 (2002).

41. Felton, S., Tolley, M., Demaine, E., Rus, D. & Wood, R. A method for building self-folding machines. *Science* **345,** 644–646 (2014).

42. Hawkes, E., An, B., Benbernou, N. M., Tanaka, H., Kim, S., Demaine, E. D., Rus, D. & Wood, R. J. Programmable matter by folding. *Proc. Natl. Acad. Sci.* **107,** 12441–12445 (2010).

43. Pratapa, P. P., Liu, K. & Paulino, G. H. Geometric mechanics of origami patterns exhibiting Poisson's ratio switch by breaking mountain and valley assignment. *Phys. Rev. Lett.* **122,** 155501 (2019).

44. Wei, Z. Y., Guo, Z. V., Dudte, L., Liang, H. Y. & Mahadevan, L. Geometric Mechanics of Periodic Pleated Origami. *Phys. Rev. Lett.* **110,** 215501 (2013).

45. Silverberg, J. L., Evans, A. A., McLeod, L., Hayward, R. C., Hull, T., Santangelo, C. D. & Cohen, I. Using origami design principles to fold reprogrammable mechanical metamaterials. *science* **345,** 647–650 (2014).

46. Liu, K., Pratapa, P. P., Misseroni, D., Tachi, T. & Paulino, G. H. Triclinic metamaterials by tristable origami with reprogrammable frustration. *Adv. Mater.* **34,** 2107998 (2022).

47. Yasuda, H. & Yang, J. Reentrant origami-based metamaterials with negative Poisson's ratio and bistability. *Phys. Rev. Lett.* **114,** 185502 (2015).

48. Waitukaitis, S., Menaut, R., Chen, B. G. & van Hecke, M. Origami Multistability: From Single Vertices to Metasheets. *Phys. Rev. Lett.* **114,** 055503 (2015).

49. Chi, Y., Li, Y., Zhao, Y., Hong, Y., Tang, Y. & Yin, J. Bistable and Multistable Actuators for Soft Robots: Structures, Materials, and Functionalities. *Adv. Mater.* **34,** 2110384 (2022).

50. Yasuda, H., Chong, C., Charalampidis, E. G., Kevrekidis, P. G. & Yang, J. Formation of rarefaction waves in origami-based metamaterials. *Phys. Rev. E* **93,** 043004 (2016).

51. Fang, H., Li, S., Ji, H. & Wang, K. W. Dynamics of a bistable Miura-origami structure. *Phys. Rev. E* **95,** 052211 (2017).

52. Dudte, L. H., Vouga, E., Tachi, T. & Mahadevan, L. Programming curvature using origami tessellations. *Nat. Mater.* **15,** 583–588 (2016).

53. Nassar, H., Lebée, A. & Monasse, L. Curvature, metric and parametrization of origami tessellations: theory and application to the eggbox pattern. *Proc. R. Soc. Math. Phys. Eng. Sci.* **473,** 20160705 (2017).

54. Liu, K. & Paulino, G. H. Nonlinear mechanics of non-rigid origami: an efficient computational approach. *Proc. R. Soc. Math. Phys. Eng. Sci.* **473,** 20170348 (2017).

55. Schenk, M. & Guest, S. D. Origami folding: A structural engineering approach. *Origami* **5,** 291–304 (2011).

56. Miyazawa, Y., Yasuda, H., Kim, H., Lynch, J. H., Tsujikawa, K., Kunimine, T., Raney, J. R. & Yang, J. Heterogeneous origami-architected materials with variable stiffness. *Commun. Mater.* **2,** 1–7 (2021).

57. Pratapa, P. P., Liu, K., Vasudevan, S. P. & Paulino, G. H. Reprogrammable Kinematic Branches in Tessellated Origami Structures. *J. Mech. Robot.* **13,** (2021).

58. Melancon, D., Gorissen, B., García-Mora, C. J., Hoberman, C. & Bertoldi, K. Multistable inflatable origami structures at the metre scale. *Nature* **592,** 545–550 (2021).

59. Novelino, L. S., Ze, Q., Wu, S., Paulino, G. H. & Zhao, R. Untethered control of functional origami microrobots with distributed actuation. *Proc. Natl. Acad. Sci.* **117,** 24096–24101 (2020).

60. Li, Y. & Yin, J. Metamorphosis of three-dimensional kirigami-inspired reconfigurable and reprogrammable architected matter. *Mater. Today Phys.* **21,** 100511 (2021).

61. Misseroni, D., Pratapa, P. P., Liu, K. & Paulino, G. H. Experimental realization of tunable Poisson's ratio in deployable origami metamaterials. *Extreme Mech. Lett.* **53,** 101685 (2022).

62. Miura, K. & Lang, R. J. The science of Miura-ori: A review. *Origami* **4,** 87–99 (2009).

63. Nauroze, S. A., Novelino, L. S., Tentzeris, M. M. & Paulino, G. H. Continuous-range tunable multilayer frequency-selective surfaces using origami and inkjet printing. *Proc. Natl. Acad. Sci.* **115,** 13210–13215 (2018).

64. Sareh, P., Chermprayong, P., Emmanuelli, M., Nadeem, H. & Kovac, M. Rotorigami: A rotary origami protective system for robotic rotorcraft. *Sci. Robot.* **3,** eaah5228 (2018).

65. Sturm, R., Schatrow, P. & Klett, Y. Multiscale Modeling Methods for Analysis of Failure Modes in Foldcore Sandwich Panels. *Appl. Compos. Mater.* **22,** 857–868 (2015).

66. Fathers, R. K., Gattas, J. M. & You, Z. Quasi-static crushing of eggbox, cube, and modified cube foldcore sandwich structures. *Int. J. Mech. Sci.* **101–102,** 421–428 (2015).

67. Hanna, B. H., Lund, J. M., Lang, R. J., Magleby, S. P. & Howell, L. L. Waterbomb base: a symmetric single-vertex bistable origami mechanism. *Smart Mater. Struct.* **23,** 094009 (2014).

68. Fonseca, L. M. & Savi, M. A. Nonlinear dynamics of an autonomous robot with deformable origami wheels. *Int. J. Non-Linear Mech.* **125,** 103533 (2020).

69. Lee, D.-Y., Kim, J.-K., Sohn, C.-Y., Heo, J.-M. & Cho, K.-J. High–load capacity origami transformable wheel. *Sci. Robot.* **6,** eabe0201 (2021).

70. Kuribayashi, K., Tsuchiya, K., You, Z., Tomus, D., Umemoto, M., Ito, T. & Sasaki, M. Self-deployable origami stent grafts as a biomedical application of Ni-rich TiNi shape memory alloy foil. *Mater. Sci. Eng. A* **419,** 131–137 (2006).

71. Chudoba, R., van der Woerd, J., Schmerl, M. & Hegger, J. ORICRETE: Modeling support for design and manufacturing of folded concrete structures. *Adv. Eng. Softw.* **72,** 119–127 (2014).

72. Kaufmann, J., Bhovad, P. & Li, S. Harnessing the multistability of Kresling origami for reconfigurable articulation in soft robotic arms. *Soft Robot.* **9,** 212–223 (2022).

73. Evans, T. A., Lang, R. J., Magleby, S. P. & Howell, L. L. Rigidly foldable origami gadgets and tessellations. *R. Soc. Open Sci.* **2,** 150067 (2015).

74. Lang, R. J., Magleby, S. & Howell, L. Single Degree-of-Freedom Rigidly Foldable Cut Origami Flashers. *J. Mech. Robot.* **8,** (2016).

75. Chen, Z., Wu, T., Nian, G., Shan, Y., Liang, X., Jiang, H. & Qu, S. Ron Resch Origami Pattern Inspired Energy Absorption Structures. *J. Appl. Mech.* **86,** (2018).

76. Kim, W., Byun, J., Kim, J.-K., Choi, W.-Y., Jakobsen, K., Jakobsen, J., Lee, D.-Y. & Cho, K.-J. Bioinspired dual-morphing stretchable origami. *Sci. Robot.* **4,** eaay3493 (2019).

77. Overvelde, J. T. B., Weaver, J. C., Hoberman, C. & Bertoldi, K. Rational design of reconfigurable prismatic architected materials. *Nature* **541,** 347–352 (2017).

78. Babaee, S., Overvelde, J. T. B., Chen, E. R., Tournat, V. & Bertoldi, K. Reconfigurable origami-inspired acoustic waveguides. *Sci. Adv.* **2,** e1601019 (2016).

79. Lu, L., Dang, X., Feng, F., Lv, P. & Duan, H. Conical Kresling origami and its applications to curvature and energy programming. *Proc. R. Soc. A* **478,** 20210712 (2022).

80. Silverberg, J. L., Na, J.-H., Evans, A. A., Liu, B., Hull, T. C., Santangelo, C. D., Lang, R. J., Hayward, R. C. & Cohen, I. Origami structures with a critical transition to bistability arising from hidden degrees of freedom. *Nat. Mater.* **14,** 389–393 (2015).

81. Filipov, E. T., Tachi, T. & Paulino, G. H. Origami tubes assembled into stiff, yet reconfigurable structures and metamaterials. *Proc. Natl. Acad. Sci.* **112,** 12321–12326 (2015).

82. Jamalimehr, A., Mirzajanzadeh, M., Akbarzadeh, A. & Pasini, D. Rigidly flat-foldable class of lockable origami-inspired metamaterials with topological stiff states. *Nat. Commun.* **13,** 1816 (2022).

83. Zhai, Z., Wang, Y. & Jiang, H. Origami-inspired, on-demand deployable and collapsible mechanical metamaterials with tunable stiffness. *Proc. Natl. Acad. Sci.* **115,** 2032–2037 (2018).

84. Yasuda, H., Tachi, T., Lee, M. & Yang, J. Origami-based tunable truss structures for non-volatile mechanical memory operation. *Nat. Commun.* **8,** 962 (2017).

85. Kotikian, A., McMahan, C., Davidson, E. C., Muhammad, J. M., Weeks, R. D., Daraio, C. & Lewis, J. A. Untethered soft robotic matter with passive control of shape morphing and propulsion. *Sci. Robot.* **4,** eaax7044 (2019).

86. Mintchev, S., Shintake, J. & Floreano, D. Bioinspired dual-stiffness origami. Science Robotics, 3 (20): eaau0275. (2018).

87. Pratapa, P. P., Suryanarayana, P. & Paulino, G. H. Bloch wave framework for structures with nonlocal interactions: Application to the design of origami acoustic metamaterials. *J. Mech. Phys. Solids* **118,** 115–132 (2018).

88. Yasuda, H., Miyazawa, Y., Charalampidis, E. G., Chong, C., Kevrekidis, P. G. & Yang, J. Origami-based impact mitigation via rarefaction solitary wave creation. *Sci. Adv.* **5,** eaau2835 (2019).

89. Lang, R. J. & Twists, T. Tessellations: Mathematical Methods for Geometric Origami. (2017).

90. Liu, K., Novelino, L. S., Gardoni, P. & Paulino, G. H. Big influence of small random imperfections in origami-based metamaterials. *Proc. R. Soc. A* **476,** 20200236 (2020).

91. Xia, Y., Kidambi, N., Filipov, E. & Wang, K.-W. Deployment dynamics of Miura origami sheets. *J. Comput. Nonlinear Dyn.* **17,** 071005 (2022).

92. Mora, S., Pugno, N. M. & Misseroni, D. 3D printed architected lattice structures by material jetting. *Mater. Today* 107–132 (2022).

93. Melancon, D., Forte, A. E., Kamp, L. M., Gorissen, B. & Bertoldi, K. Inflatable origami: Multimodal deformation via multistability. *Adv. Funct. Mater.* **32,** 2201891 (2022).

94. Mehrpouya, M., Azizi, A., Janbaz, S. & Gisario, A. Investigation on the functionality of thermoresponsive origami structures. *Adv. Eng. Mater.* **22,** 2000296 (2020).

95. Dalaq, A. S. & Daqaq, M. F. Experimentally-validated computational modeling and characterization of the quasi-static behavior of functional 3D-printed origami-inspired springs. *Mater. Des.* **216,** 110541 (2022).

96. Huang, C., Tan, T., Hu, X., Yang, F. & Yan, Z. Bio-inspired programmable multi-stable origami. *Appl. Phys. Lett.* **121,** 051902 (2022).

97. Qi, J., Li, C., Tie, Y., Zheng, Y. & Duan, Y. Energy absorption characteristics of origami-inspired honeycomb sandwich structures under low-velocity impact loading. *Mater. Des.* **207,** 109837 (2021).

98. Cheung, K. C., Tachi, T., Calisch, S. & Miura, K. Origami interleaved tube cellular materials. *Smart Mater. Struct.* **23,** 094012 (2014).

99. Zhao, Z., Kuang, X., Wu, J., Zhang, Q., Paulino, G. H., Qi, H. J. & Fang, D. 3D printing of complex origami assemblages for reconfigurable structures. *Soft Matter* **14,** 8051–8059 (2018).

100. Zhao, Z., Wu, J., Mu, X., Chen, H., Qi, H. J. & Fang, D. Origami by frontal photopolymerization. *Sci. Adv.* **3,** e1602326 (2017).

101. Lin, Z., Novelino, L. S., Wei, H., Alderete, N. A., Paulino, G. H., Espinosa, H. D. & Krishnaswamy, S. Folding at the microscale: Enabling multifunctional 3D origami-architected metamaterials. *Small* **16,** 2002229 (2020).

102. Fang, Z., Song, H., Zhang, Y., Jin, B., Wu, J., Zhao, Q. & Xie, T. Modular 4D Printing via Interfacial

Welding of Digital Light-Controllable Dynamic Covalent Polymer Networks. *Matter* **2,** 1187–1197 (2020).

103. Ge, Q., Dunn, C. K., Qi, H. J. & Dunn, M. L. Active origami by 4D printing. *Smart Mater. Struct.* **23,** 094007 (2014).

104. Xia, X., Spadaccini, C. M. & Greer, J. R. Responsive materials architected in space and time. *Nat. Rev. Mater.* **7,** 683–701 (2022).

105. Chen, T., Bilal, O. R., Lang, R., Daraio, C. & Shea, K. Autonomous Deployment of a Solar Panel Using Elastic Origami and Distributed Shape-Memory-Polymer Actuators. *Phys. Rev. Appl.* **11,** 064069 (2019).

106. Sitti, M. *Mobile microrobotics*. (MIT Press, 2017).

107. Cui, J., Huang, T.-Y., Luo, Z., Testa, P., Gu, H., Chen, X.-Z., Nelson, B. J. & Heyderman, L. J. Nanomagnetic encoding of shape-morphing micromachines. *Nature* **575,** 164–168 (2019).

108. Thota, M. & Wang, K. W. Reconfigurable origami sonic barriers with tunable bandgaps for traffic noise mitigation. *J. Appl. Phys.* **122,** 154901 (2017).

109. Boatti, E., Vasios, N. & Bertoldi, K. Origami metamaterials for tunable thermal expansion. *Adv. Mater.* **29,** 1700360 (2017).

110. Mukhopadhyay, T., Ma, J., Feng, H., Hou, D., Gattas, J. M., Chen, Y. & You, Z. Programmable stiffness and shape modulation in origami materials: Emergence of a distant actuation feature. *Appl. Mater. Today* **19,** 100537 (2020).

111. Kobayashi, H., Kresling, B. & Vincent, J. F. V. The geometry of unfolding tree leaves. *Proc. R. Soc. Lond. B Biol. Sci.* **265,** 147–154 (1998).

112. Chen, Y., Feng, H., Ma, J., Peng, R. & You, Z. Symmetric waterbomb origami. *Proc. R. Soc. Math. Phys. Eng. Sci.* **472,** 20150846 (2016).

113. Randlett, S. The Art of Origami: Paper Folding. *Tradit. Mod. EP Dutton* (1961).

114. Pratapa, P. P. & Bellamkonda, A. Thick panel origami for load-bearing deployable structures. *Mech. Res. Commun.* **124,** 103937 (2022).

115. Vasudevan, S. P. & Pratapa, P. P. Origami metamaterials with near-constant Poisson functions over finite strains. *J. Eng. Mech.* **147,** 04021093 (2021).

116. Moshtaghzadeh, M., Izadpanahi, E. & Mardanpour, P. Prediction of fatigue life of a flexible foldable origami antenna with Kresling pattern. *Eng. Struct.* **251,** 113399 (2022).

117. Tang, J. & Wei, F. Miniaturized Origami Robots: Actuation Approaches and Potential Applications. *Macromol. Mater. Eng.* **307,** 2100671 (2022).

118. Thota, M. & Wang, K. W. Tunable waveguiding in origami phononic structures. *J. Sound Vib.* **430,** 93–100 (2018).

119. Tang, R., Huang, H., Tu, H., Liang, H., Liang, M., Song, Z., Xu, Y., Jiang, H. & Yu, H. Origami-enabled deformable silicon solar cells. *Appl. Phys. Lett.* **104,** 083501 (2014).

120. Li, S., Vogt, D. M., Rus, D. & Wood, R. J. Fluid-driven origami-inspired artificial muscles. *Proc.*

Natl. Acad. Sci. **114,** 13132–13137 (2017).

121. McClintock, H., Temel, F. Z., Doshi, N., Koh, J. & Wood, R. J. The milliDelta: A high-bandwidth, high-precision, millimeter-scale Delta robot. *Sci. Robot.* **3,** eaar3018 (2018).

122. Wang, C., Guo, H., Liu, R. & Deng, Z. A programmable origami-inspired space deployable structure with curved surfaces. *Eng. Struct.* **256,** 113934 (2022).

123. Gabler, F., Karnaushenko, D. D., Karnaushenko, D. & Schmidt, O. G. Magnetic origami creates high performance micro devices. *Nat. Commun.* **10,** 3013 (2019).

124. Velvaluri, P., Soor, A., Plucinsky, P., de Miranda, R. L., James, R. D. & Quandt, E. Origami-inspired thin-film shape memory alloy devices. *Sci. Rep.* **11,** 10988 (2021).

125. Taghavi, M., Helps, T. & Rossiter, J. Electro-ribbon actuators and electro-origami robots. *Sci. Robot.* **3,** eaau9795 (2018).

126. Reis, P. M., López Jiménez, F. & Marthelot, J. Transforming architectures inspired by origami. *Proc. Natl. Acad. Sci.* **112,** 12234–12235 (2015).

127. Pesenti, M., Masera, G. & Fiorito, F. Exploration of Adaptive Origami Shading Concepts through Integrated Dynamic Simulations. *J. Archit. Eng.* **24,** 04018022 (2018).

128. Le-Thanh, L., Le-Duc, T., Ngo-Minh, H., Nguyen, Q.-H. & Nguyen-Xuan, H. Optimal design of an Origami-inspired kinetic façade by balancing composite motion optimization for improving daylight performance and energy efficiency. *Energy* **219,** 119557 (2021).

129. Miranda, R., Babilio, E., Singh, N., Santos, F. & Fraternali, F. Mechanics of smart origami sunscreens with energy harvesting ability. *Mech. Res. Commun.* **105,** 103503 (2020).

130. Babilio, E., Miranda, R. & Fraternali, F. On the Kinematics and Actuation of Dynamic Sunscreens With Tensegrity Architecture. *Front. Mater.* **6,** (2019).

131. Attia, S. Evaluation of adaptive facades: The case study of Al Bahr Towers in the UAE. *QScience Connect* **2017,** 6 (2018).

132. Xu, Y., Ma, J., Liu, D., Xu, H., Cui, F. & Wang, W. Origami system for efficient solar driven distillation in emergency water supply. *Chem. Eng. J.* **356,** 869–876 (2019).

133. Zirbel, S. A., Trease, B. P., Thomson, M. W., Lang, R. J., Magleby, S. P. & Howell, L. H. HanaFlex: a large solar array for space applications. in *Micro- Nanotechnol. Sens. Syst. Appl. VII* **9467,** 179–187 (SPIE, 2015).

134. Klett, Y., Middendorf, P., Sobek, W., Haase, W. & Heidingsfeld, M. Potential of origami-based shell elements as next-generation envelope components. in *2017 IEEE Int. Conf. Adv. Intell. Mechatron. AIM* 916–920 (2017).

135. Quaglia, C. P., Yu, N., Thrall, A. P. & Paolucci, S. Balancing energy efficiency and structural performance through multi-objective shape optimization: Case study of a rapidly deployable origami-inspired shelter. *Energy Build.* **82,** 733–745 (2014).

136. Lee, T.-U. & Gattas, J. M. Geometric Design and Construction of Structurally Stabilized Accordion Shelters. *J. Mech. Robot.* **8,** (2016).

137. Kadic, M., Milton, G. W., van Hecke, M. & Wegener, M. 3D metamaterials. *Nat. Rev. Phys.* **1,**

198–210 (2019).

138. Bertoldi, K., Vitelli, V., Christensen, J. & Van Hecke, M. Flexible mechanical metamaterials. *Nat. Rev. Mater.* **2,** 1–11 (2017).

139. Zhang, Q., Wang, X., Cai, J. & Feng, J. Motion paths and mechanical behavior of origami-inspired tunable structures. *Mater. Today Commun.* **26,** 101872 (2021).

140. Lee, T.-U., Chen, Y., Heitzmann, M. T. & Gattas, J. M. Compliant curved-crease origami-inspired metamaterials with a programmable force-displacement response. *Mater. Des.* **207,** 109859 (2021).

141. Feng, H., Peng, R., Zang, S., Ma, J. & Chen, Y. Rigid foldability and mountain-valley crease assignments of square-twist origami pattern. *Mech. Mach. Theory* **152,** 103947 (2020).

142. Saito, K., Tsukahara, A. & Okabe, Y. Designing of self-deploying origami structures using geometrically misaligned crease patterns. *Proc. R. Soc. Math. Phys. Eng. Sci.* **472,** 20150235 (2016).

143. Zhai, Z., Wang, Y., Lin, K., Wu, L. & Jiang, H. In situ stiffness manipulation using elegant curved origami. *Sci. Adv.* **6,** eabe2000 (2020).

144. Zhai, Z., Wu, L. & Jiang, H. Mechanical metamaterials based on origami and kirigami. *Appl. Phys. Rev.* **8,** 041319 (2021).

145. Kamrava, S., Mousanezhad, D., Ebrahimi, H., Ghosh, R. & Vaziri, A. Origami-based cellular metamaterial with auxetic, bistable, and self-locking properties. *Sci. Rep.* **7,** 1–9 (2017).

146. Zhao, S., Zhang, Y., Zhang, Y., Yang, J. & Kitipornchai, S. Graphene origami-enabled auxetic metallic metamaterials: an atomistic insight. *Int. J. Mech. Sci.* **212,** 106814 (2021).

147. Fang, H., Chu, S.-C. A., Xia, Y. & Wang, K.-W. Programmable self-locking origami mechanical metamaterials. *Adv. Mater.* **30,** 1706311 (2018).

148. Pinson, M. B., Stern, M., Carruthers Ferrero, A., Witten, T. A., Chen, E. & Murugan, A. Self-folding origami at any energy scale. *Nat. Commun.* **8,** 15477 (2017).

149. Tolman, S. S., Delimont, I. L., Howell, L. L. & Fullwood, D. T. Material selection for elastic energy absorption in origami-inspired compliant corrugations. *Smart Mater. Struct.* **23,** 094010 (2014).

150. Wen, G., Chen, G., Long, K., Wang, X., Liu, J. & Xie, Y. M. Stacked-origami mechanical metamaterial with tailored multistage stiffness. *Mater. Des.* **212,** 110203 (2021).

151. Ma, J., Song, J. & Chen, Y. An origami-inspired structure with graded stiffness. *Int. J. Mech. Sci.* **136,** 134–142 (2018).

152. Wang, Z., Jing, L., Yao, K., Yang, Y., Zheng, B., Soukoulis, C. M., Chen, H. & Liu, Y. Origami-Based Reconfigurable Metamaterials for Tunable Chirality. *Adv. Mater.* **29,** 1700412 (2017).

153. Xu, X., He, S., Wang, C., Chen, X., Wang, Z. & Song, J. Origami-Inspired Chiral Metamaterials With Tunable Circular Dichroism Through Mechanically Guided Three-Dimensional Assembly. *J. Appl. Mech.* **90,** (2022).

154. Li, M., Shen, L., Jing, L., Xu, S., Zheng, B., Lin, X., Yang, Y., Wang, Z. & Chen, H. Origami Metawall: Mechanically Controlled Absorption and Deflection of Light. *Adv. Sci.* **6,** 1901434 (2019).

155. Ji, J. C., Luo, Q. & Ye, K. Vibration control based metamaterials and origami structures: A state-

of-the-art review. *Mech. Syst. Signal Process.* **161,** 107945 (2021).

156. Fuchi, K., Diaz, A. R., Rothwell, E. J., Ouedraogo, R. O. & Tang, J. An origami tunable metamaterial. *J. Appl. Phys.* **111,** 084905 (2012).

157. Zhao, P., Zhang, K. & Deng, Z. Origami-inspired lattice for the broadband vibration attenuation by Symplectic method. *Extreme Mech. Lett.* **54,** 101771 (2022).

158. Feng, H., Ma, J., Chen, Y. & You, Z. Twist of Tubular Mechanical Metamaterials Based on Waterbomb Origami. *Sci. Rep.* **8,** 9522 (2018).

159. Wu, S., Ze, Q., Dai, J., Udipi, N., Paulino, G. H. & Zhao, R. Stretchable origami robotic arm with omnidirectional bending and twisting. *Proc. Natl. Acad. Sci.* **118,** e2110023118 (2021).

160. Hines, L., Petersen, K., Lum, G. Z. & Sitti, M. Soft Actuators for Small-Scale Robotics. *Adv. Mater.* **29,** 1603483 (2017).

161. Jiang, Y., Li, Y., Liu, K., Zhang, H., Tong, X., Chen, D., Wang, L. & Paik, J. Ultra-tunable bistable structures for universal robotic applications. *Cell Rep. Phys. Sci.* **4,** 101365 (2023).

162. Jiang, H., Wang, Z., Jin, Y., Chen, X., Li, P., Gan, Y., Lin, S. & Chen, X. Hierarchical control of soft manipulators towards unstructured interactions. *Int. J. Robot. Res.* **40,** 411–434 (2021).

163. Lee, J.-G. & Rodrigue, H. Origami-Based Vacuum Pneumatic Artificial Muscles with Large Contraction Ratios. *Soft Robot.* **6,** 109–117 (2019).

164. Lin, Y., Yang, G., Liang, Y., Zhang, C., Wang, W., Qian, D., Yang, H. & Zou, J. Controllable Stiffness Origami "Skeletons" for Lightweight and Multifunctional Artificial Muscles. *Adv. Funct. Mater.* **30,** 2000349 (2020).

165. Johnson, M., Chen, Y., Hovet, S., Xu, S., Wood, B., Ren, H., Tokuda, J. & Tse, Z. T. H. Fabricating biomedical origami: a state-of-the-art review. *Int. J. Comput. Assist. Radiol. Surg.* **12,** 2023–2032 (2017).

166. Randall, C. L., Gultepe, E. & Gracias, D. H. Self-folding devices and materials for biomedical applications. *Trends Biotechnol.* **30,** 138–146 (2012).

167. Taylor, A. J., Xu, S., Wood, B. J. & Tse, Z. T. H. Origami Lesion-Targeting Device for CT-Guided Interventions. *J. Imaging* **5,** 23 (2019).

168. Taylor, A., Miller, M., Fok, M., Nilsson, K. & Tsz Ho Tse, Z. Intracardiac Magnetic Resonance Imaging Catheter With Origami Deployable Mechanisms1. *J. Med. Devices* **10,** (2016).

169. Kim, S.-J., Lee, D.-Y., Jung, G.-P. & Cho, K.-J. An origami-inspired, self-locking robotic arm that can be folded flat. *Sci. Robot.* **3,** eaar2915 (2018).

170. Banerjee, H., Li, T. K., Ponraj, G., Kirthika, S. K., Lim, C. M. & Ren, H. Origami-Layer-Jamming Deployable Surgical Retractor With Variable Stiffness and Tactile Sensing. *J. Mech. Robot.* **12,** (2020).

171. Bobbert, F. S. L., Janbaz, S., van Manen, T., Li, Y. & Zadpoor, A. A. Russian doll deployable meta-implants: Fusion of kirigami, origami, and multi-stability. *Mater. Des.* **191,** 108624 (2020).

172. Yang, N., Deng, Y., Mao, Z. F., Chen, Y. T., Wu, N. & Niu, X. D. New network architectures with tunable mechanical properties inspired by origami. *Mater. Today Adv.* **4,** 100028 (2019).

173. Prabhakar, S., Singh, J. P., Roy, D. & Prasad, N. E. Stable 3D hierarchical scaffolds by origami approach: Effect of interfacial crosslinking by nanohybrid shish-kebab assemblies. *Mater. Des.* **213,** 110353 (2022).

174. Kim, S.-H., Lee, H. R., Yu, S. J., Han, M.-E., Lee, D. Y., Kim, S. Y., Ahn, H.-J., Han, M.-J., Lee, T.-I., Kim, T.-S., Kwon, S. K., Im, S. G. & Hwang, N. S. Hydrogel-laden paper scaffold system for origami-based tissue engineering. *Proc. Natl. Acad. Sci.* **112,** 15426–15431 (2015).

175. Chauhan, M., Chandler, J. H., Jha, A., Subramaniam, V., Obstein, K. L. & Valdastri, P. An Origami-Based Soft Robotic Actuator for Upper Gastrointestinal Endoscopic Applications. *Front. Robot. AI* **8,** (2021).

176. Zhu, S. & Li, T. Hydrogenation-Assisted Graphene Origami and Its Application in Programmable Molecular Mass Uptake, Storage, and Release. *ACS Nano* **8,** 2864–2872 (2014).

177. Suzuki, H. & Wood, R. J. Origami-inspired miniature manipulator for teleoperated microsurgery. *Nat. Mach. Intell.* **2,** 437–446 (2020).

178. Sargent, B., Butler, J., Seymour, K., Bailey, D., Jensen, B., Magleby, S. & Howell, L. An Origami-Based Medical Support System to Mitigate Flexible Shaft Buckling. *J. Mech. Robot.* **12,** (2020).

179. Leong, T. G., Randall, C. L., Benson, B. R., Bassik, N., Stern, G. M. & Gracias, D. H. Tetherless thermobiochemically actuated microgrippers. *Proc. Natl. Acad. Sci.* **106,** 703–708 (2009).

180. Ghosh, A., Yoon, C., Ongaro, F., Scheggi, S., Selaru, F. M., Misra, S. & Gracias, D. H. Stimuli-Responsive Soft Untethered Grippers for Drug Delivery and Robotic Surgery. *Front. Mech. Eng.* **3,** (2017).

181. Natori, M. C., Sakamoto, H., Katsumata, N., Yamakawa, H. & Kishimoto, N. Conceptual model study using origami for membrane space structures-a perspective of origami-based engineering. *Mech. Eng. Rev.* **2,** 14–00368 (2015).

182. Miura, K. & Pellegrino, S. *Forms and concepts for lightweight structures*. (Cambridge University Press, 2020).

183. Miura, K. Method of packaging and deployment of large membranes in space. *Inst. Space Astronaut. Sci. Rep.* **618,** 1–9 (1985).

184. Miura, K. Concepts of Deployable Space Structures. *Int. J. Space Struct.* **8,** 3–16 (1993).

185. Guest, S. D. & Pellegrino, S. Inextensional wrapping of flat membranes. in *Proc. First Int. Semin. Struct. Morphol.* **25,** (1992).

186. De Focatiis, D. S. A. & Guest, S. D. Deployable membranes designed from folding tree leaves. *Philos. Trans. R. Soc. Lond. Ser. Math. Phys. Eng. Sci.* **360,** 227–238 (2002).

187. Parque, V., Suzaki, W., Miura, S., Torisaka, A., Miyashita, T. & Natori, M. Packaging of thick membranes using a multi-spiral folding approach: Flat and curved surfaces. *Adv. Space Res.* **67,** 2589–2612 (2021).

188. Wilson, L., Pellegrino, S. & Danner, R. Origami sunshield concepts for space telescopes. in *54th AIAAASMEASCEAHSASC Struct. Struct. Dyn. Mater. Conf.* 1594 (2013).

189. Wasserthal, L. T. The open hemolymph system of Holometabola and its relation to the tracheal

space. *Microsc. Anat. Invertebr.* **11,** 583–620 (1998).

190. Kersten, M., Kling, G. & Burkhardt, J. IXO telescope mirror design and its performance. in *Int. Conf. Space Opt. 2010* **10565,** 769–775 (SPIE, 2019).

191. Tachi, T. Design of infinitesimally and finitely flexible origami based on reciprocal figures. *J Geom Graph* **16,** 223–234 (2012).

192. Ghassaei, A., Demaine, E. D. & Gershenfeld, N. Fast, interactive origami simulation using GPU computation, Origami, 7: 1151-1166. (2018).

193. Demaine, E. D., Ku, J. S. & Lang, R. J. A new file standard to represent folded structures. in *Abstr 26th Fall Workshop Comput. Geom.* 27–28 (2016).

194. Hu, Y., Zhou, Y. & Liang, H. Constructing rigid-foldable generalized Miura-ori tessellations for curved surfaces. *J. Mech. Robot.* **13,** (2021).

195. Dudte, L. H., Choi, G. P. & Mahadevan, L. An additive algorithm for origami design. *Proc. Natl. Acad. Sci.* **118,** e2019241118 (2021).

196. Dang, X., Feng, F., Plucinsky, P., James, R. D., Duan, H. & Wang, J. Inverse design of deployable origami structures that approximate a general surface. *Int. J. Solids Struct.* **234,** 111224 (2022).

197. Ze, Q., Wu, S., Nishikawa, J., Dai, J., Sun, Y., Leanza, S., Zemelka, C., Novelino, L. S., Paulino, G. H. & Zhao, R. R. Soft robotic origami crawler. *Sci. Adv.* **8,** eabm7834 (2022).

198. Fernandes, R. & Gracias, D. H. Self-folding polymeric containers for encapsulation and delivery of drugs. *Adv. Drug Deliv. Rev.* **64,** 1579–1589 (2012).